EVALUATION OF CdX (X = S, Se) QUANTUM DOTS AS PHOTOINITIATOR IN FREE RADICAL POLYMERIZATIONS

by

Enes Buz

A Thesis Submitted to the

Graduate School of Sciences and Engineering

in Partial Fulfillment of the Requirements for

the Degree of

Master of Science

in

Material Science and Engineering

Koc University

August 2017

Koc University

Graduate School of Sciences and Engineering

This is to certify that I have examined this copy of a M.S. thesis by

Enes Buz

and have found that it is complete and satisfactory in all respects,

and that any and all revisions required by the final

examining committee have been made.

Committee Members:

_____

Havva F. Yağcı Acar, Ph. D. (Advisor)

_____

Uğur Ünal, Ph. D.

_____

Duygu Avcı, Ph. D.

Date: _____

Abstract

Free radical photopolymerization of vinyl monomers is highly popular since initiation can be performed at room temperature which is beneficial in especially medicine, paint and coating applications. Photoinitiators (PI) usually do have strong absorbance in the UV and therefore decompose to produce free radicals for initiation upon excitation in UV which creates a safety issue and limited penetration depth. Lack of 100% decomposition, toxicity of the PI and/or degradation products, bleaching out of these species and need for a co-catalyst are additional problems which are the subjects of many current studies.

Quantum dots (QD) are luminescent semiconductor nanocrystals with size tunable optical and electrical properties due to quantum confinement and used widely in energy, medicine, fluorescent labeling, optical diagnosis and therapy. Their combination with polymers usually involve polymeric coatings on QDs to provide stability, functionalization and processability to QDs or blending QDs with polymers to introduce the optical and electrical properties of QDs to the polymers.

QDs generate an electron-hole pair which is the basis of their potential as a PI. Size tunable and continues absorbance of QDs allow excitation at different wavelength and hence render them as a potential long-wavelength initiators. There has been a very limited amount of reports on utilization of QDs as PIs within the last 20. Results of these studies are usually conflicting with each other. General belief involves the need for a hole-scavenging alcoholic solvent and luminescence quenching for successful photoinitiation with QDs.

Motivation of this thesis work is four fold: 1. Understanding of the influence of QD type, size, surface quality and coating composition on PI efficiency in hydrophobic solvents; 2. Elucidating the initiation mechanism; 3. Investigating QDs as long-wavelength PIs; 4. Producing QD/polymer nanocomposites in a simple way.

In the first part, colloidal and hydrophobic CdS QDs with different crystal size and particle quality, but with the same coating (oleic acid) were used as a PI in batch photopolymerization of MMA under UV-excitation (360 nm) wherein the QD concentration and reaction time on monomer conversion were studied. Kinetics of the photopolymerization and initiation in the visible range were studied with photo-DSC using PEGDA and HDDA as monomers. Studies indicate that more than the size of the nanocrystals, surface quality and defect states differentiate the initiation efficiency of QDs. Small, colloidally stable and luminescent CdS/PMMA were produced. Decarboxylation of Oleic acid upon photoexcitation was suggested as the source of initiating radical. In the second part, octadecylamine coated CdSe and CdSe-ZnS core-shell QDs were studied to shed

light on the initiation mechanism further. However, successful photopolymerization were not achieved. Possible reasons and suggestions for future studies are provided in the last part.

Özet

Vinil monomerlerinin serbest radikal polimerizasyonu tekniği ile polimerleştirilmesi özellikle tıp, boya, kaplama sahalarında, özellikle de oda sıcaklığında çalışma avantajı sağladığı için, çokça başvurulan bir yöntemdir. Fotobaşlatıcılar (FB) genellikle UV-bölgesinde absorbansa sahip ve dolayısıyla UV-de uyarıldıklarında radikal oluşturarak parçalanıp polimerizasyon başlatan organik moleküllerdir. UV ışığının kullanılmasının sağlık açısında riskli olması ve yine bu bölgede sınırlı ışık nüfus derinliği organik FB'lerin temel sorunudur. Ayrıca, FB'ların tümüyle dönüşüme uğramaması, toksik parçalanma ürünlerinin çıkması, ko-katalist ihtiyacı organik FB'ların başlıca sorunlarıdır.

Kuantum noktacıkları (KN) kuantum sınırlaması nedeniyle büyüklüğe bağlı özellikler gösteren yarı iletken nanokristal yapılardır ve güneş pilleri, floresan etiket, ilaç taşıma ve tıbbi görüntüleme gibi pek çok sahada kullanılan popüler nanomalzemelerdir. Polimerler genellikle KN'larına stabilize, fonksiyonellik ve işlenebilirlik sağlamak için KN'larının yüzeyini kaplamada kullanılır veya KN'larının özelliklerinden faydalanmak için KN'ları ile harmanlanırlar.

KN'larının potansiyel FB olarak kullanılmasının nedeni elekron-çıkur çiftini oluşturmasıdır. KN'larının kristal büyüklüğüne bağlı değişen ve kesitli olmayan absorbansı farklı dalga boylarının uyarıcı olarak kullanılabilmesine olanak sağlar ve KN'larını olası uzun-dalgaboyu fotobaşlatıcıları haline getirir. Son yirmi yıl içerisinde kuantum

noktacıkların fotobaşlatıcı olarak kullanılabileceğine dair sınırlı sayıda raporlar görülmüştür. Genellikle de bu çalışmaların sonuncu birbiri ile çelişmektedir. Çukur-dolduran alkolik çözücülere ihtiyaç duyulması ve başarılı fotobaşlatama sonucunda luminesansın sönümlenmesi bu raporların genel görüşü olarak kabul edilebilir.

Bu tez çalışmasının motivasyonu 4 aşamalıdır: ilk olarak KN'nın tipinin, büküklüğünün, yüzey kalitesinin ve kaplama kompozisyonunun FB verimliliği üzerindeki etkisinin anlaşılması, 2. olarak başlatıcı mekanizmasının anlaşılması, 3. olarak uzun-dalgaboyu FB'si olarak değerlendirilmesi ve son olarak da basit bir yolla KN-polimer nano-kompoziti üretilmesinde kullanılması hedeflenmektedir.

Çalışmanın ilk kısmında, aynı kaplamaya fakat farklı kristal büyüklüğüne ve parçacık kalitesine sahip, kolloidal ve hidrofobik CdS KN'larının UV ışığı ile uyarılması sayesinde MMA'nın yığın polimerizasyonunda, KN'nın yoğunluğunun ve polimerizasyon süresinin MMA dönüşümündeki etkisi çalışıldı. Görünür bölgedeki başlamanın ve fotopolimerizasyon kinetiği PEGDA ve HDDA monomerleri ile foto-DSC'de çalışıldı. Elde edilen sonuçlar gösteriyor ki: KN'nın büyüklüğü, yüzeyinin kalitesi ve kusurlu enerji mevkilerini bulunması KN'larının başlatıcı verimliğini değiştirmektedir. Luminesans ve kolloidal stabilitesi olan kompozitler üretildi. Fotouyarılma sonucu oleik asitin karbondioksit açığa çıkarması başlatıcı radikalin kaynağı olarak önerildi. İkinci bölümde, çekirdek-kabuk yapılı malzemelerin fotobaşlatmadaki rolünü anlamak için oktadesilamin kaplı CdSe ve CdSe-ZnS parçacıklarından faydalanılmıştır. Fakat bu parçacıklarla başarılı sonuçlar elde edilemedi.

Son bölümde, bunun olası olası nedenleri ve ileriye yönelik yapılabilecek çalışmalara yer verildi.

Dedicated to

my dear wife and my family

Pelin Turhan Buz and Buz family

for her endless support, love

and believe in me

ACKNOWLEDGEMENT

First of all, I would like to thank my thesis advisor Assoc. Prof. Havva Funda Yağcı Acar for her guidance and support in this thesis study. Beyond the thesis, I would like to express my gratitude to her because she gave me a chance to study her laboratory when I was a junior, and from that time till now, her contribution to my life was priceless. I would like to thank my dear professor for everything.

I also would like to express my gratitude to my thesis committee members Assoc. Prof. Uğur Ünal and Prof. Duygu Avcı for their time, invaluable contributions and suggestions to my thesis. I also thank Prof. Duygu Avcı for the organic chemistry course that most likely altered my destiny and made me love chemistry. I would like to thank Assoc. Prof. Uğur Ünal one more time for his great support and help.

I would like to express my appreciation to Prof. Mehmet Somer, Prof. İskender Yılgör and Emel Yılgör for their support and invaluable contributions to my academic life. I especially thank Emel Yılgör for her kind advices, suggestions and support during Ph.D. application process and later. Besides, I would like to express my thanks to all faculty members of Materials Science and Engineering Department.

I would like to express my thanks to 'ELC tayfa': Mert Erköseoğlu, Aykut Bayram, Caner Çelik, Barış Ata, Abdullah Aydın, Ömer Akın, Burak Bastem, Kerem Çelebi' for their great friendship, support, motivation and contributions to my life. Also, I would like to thank my

dear friend and roomie İsa Özdemir for his motivation, support and invisible contributions to my life.

I would like to thank TÜBİTAK project no. 115Z463 for funding and Koc University.

I would like to thank staff of College of Science and office of Graduate School of Science and Engineering for their significant support, logistics, and contributions in the department and laboratory and especially to Ayşe Çağ Ruçoğlu for her positive welcomes in every morning and for her great coffee and tea.

I would like to thank Koc University Surface Technology Research Center (KUYTAM) for their help in characterization of QDs. I deeply appreciate the assistance and support of KUYTAM team, Dr. Barış Yağcı, Cansu, Yıldırım, Dr. Ceren Yılmaz, Assoc. Prof. Uğur Ünal.

I would like express my thanks to former and present members of Polymers and Nanomaterials Research Laboratory group, so called FUNTECH: Dr. İbrahim Hocaoğlu, Dr. Pınar Dağtepe, Dr. Yurdanur Türker, Yasemin Yar, Didar Aşık, Emre Köken, Funda Kar, Emre Nakay, Çağnur Celaloğlu, Dr. Rouhollah Khodadust, Dr. Fatma Demir Duman, Dr. Emek Göksu Durmuşoğlu, Özlem Ünal, Özge Çavuşlar, Gökay Avcı, Kübra Bilici, Mahshid Hashemkhani, Mona Nejatpour, Gözde Demirci, Aslı Çuhadar, İrem Ülkü ve Pelin Turhan Buz. I would like to express my gratitude to Dr. İbrahim Hocaoglu ve Dr. Rouhollah Khodadust for their sincere advices and for their behavior to me like they are my big brothers.

Many thanks to my all colleagues and friends in the Chemistry department and other departments: Özgün Önder Can, Tuğçe Beyazay, Merve Aksoy, Feriha Eylül Saraç, Çiğdem Altıntaş, Dr. Benay Uzer, Kübra Sarı, Kamil Kiraz, İrem Mağazacı, Günce Sıdıka Yıldırım.

I am also greatly indebted to my GANG and Harry Potter team: Özge Çavuşlar, İrem Ülkü and Gökay Avcı. They made my master years great, and were always there for me to listen, motivate and support. I would like to sincerely thank all of you for these 2 great years. Also, I would like to express my special thanks to Özlem Ünal for her unique friendship and for her endless support.

I would like to express my thanks to my oldies but goldies: Dr. Ömer Faruk Şimşek, Abdurrahman Dinç and Ronay Çetin for their great contributions to my life ad being always with me.

Finally, I would like to express my sincere thanks to my wife Pelin Turhan Buz and big family to whom I dedicated my thesis study. I am very grateful to my mother Zehra Buz and my father İbrahim Buz for their everlasting support, trust, encouragement, motivation, financial and spiritual support. I am thankful to my beloved wife for her endless support, motivation, love. Also, I thank my brothers Esat Buz and Muhammed Buz for their love and motivation, thank to my nephew for his help and support, and special thanks to my new family: Fahrettin Turhan, Nuray Turhan, Beril Turhan and Arda Hacırecepoğlu.

Table of Contents

List of Figures

List of Tables

List of Schemes

Nomenclature

CB	Conduction Band
CdS	Cadmium Sulfide
CdSe	Cadmium Selenide
DSC	Differential Scanning Calorimetry
EBR	Exciton Bohr Radius
E_g	Bandgap Energy
eV	Electron Volt
FRP	Free Radical Polymerization
HDDA	1,6-hexanediol diacrylate
MMA	Methyl methacrylate
M_n	Number average molecular weight
NC	Nanocrystal
NP	Nanoparticle
OA	Oleic Acid
ODA	Octadecylamine
1-ODE	1-octadecene
PEGDA	Poly(ethylene glycol) diacrylate
PI	Photoinitiator
PL	Photoluminescence
QD	Quantum Dot
QY	Quantum Yield
TAA	Thioacetamide

TEA	Triethylamine
T_g	Glass transition temperature
VB	Valence Band
ZnO	Zinc oxide

1. Introduction

1.1 Quantum Dots

Nanoparticles have become a center of attention within almost all fields of science and technology. Among different inorganic nanoparticles, Quantum Dots (QDs) emerged as a valuable enabling material in a variety of applications. They did not only initiate a tremendous amount of fundamental research but also were utilized in new technology products and even made it to the market. QDs are luminescent semiconducting nanocrystals with diameters usually in the range of 2-10 nm (**Figure 1.1**).[1] Such ultra-small size dramatically alters their physical, chemical and optical properties, providing outstanding features valuable for different applications including solar cells[2, 3], bio-imaging[4, 5], displays[6], photocatalysis[7, 8], sensors[9], etc. QDs are synthesized from the elements of group II-VI (i.e. CdS, CdTe), IV-VI (i.e. PbS) or III-V (i.e. InGa) elements.

Figure 1.1 Ten different colors of fluorescent ZnS-CdSe QDs under near UV light [10]

1.1.1 Size-Band Gap Relation

Solid state materials are classified as conductors (or metals), semiconductors or insulators based on materials' electronic band structures (**Figure 1.2**). Conductors are good conductors of electricity and heat as a consequence of their continuous energy bands or very small gap between the valence band (VB) and the conduction band (CB), which can be readily overcomed even at the room temperature. On the other hand, insulators have a large energy band gap (usually larger than 3.0 electron volts (eV)) or forbidden energy levels. In the case of semiconductors, such energy band gap is relatively smaller.

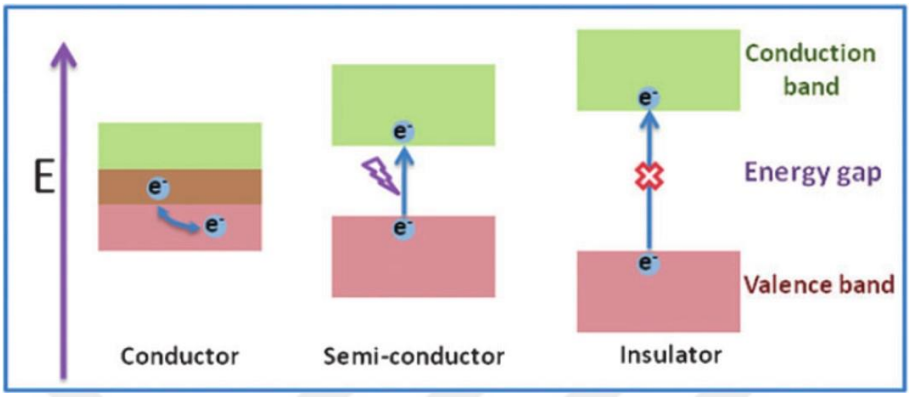

Figure 1.2 Electronic band structures of inorganic solids[5]

A bulk semiconductor contains many atoms which cause splitting of the electronic energy levels, and as a consequence, continuous energy bands form in a bulk semiconductor (**Figure 1.3**). [11] A semiconductor crystal possesses quantum mechanically calculated forbidden energy zone that is also referred as the *band gap energy* (E_g), and it is specific to the material. **Table 1.1** shows bulk band gap energies of most widely studied QDs in the literature.[12] The valance band is the mostly filled lower-energy band while conduction band is the mostly empty higher energy band.

Table 1.1 Band-gap energies of commonly used semiconductors [12]

Bulk semiconductor	Band Gap [eV]	Type
CdS	2.42	II-VI
CdSe	1.75	II-VI
CdTe	1.50	II-VI
InP	1.35	III-V
PbS	0.41	IV-VI
ZnS	2.50	II-VI

Electrons located in the valence band can be promoted to the conduction band only when they are excited with an energy equal or greater than the band gap of the material. Excitation of an electron from its ground state to a higher energy levels leaves a positively charged hole behind and allocates the negatively charged electron in the conduction band. Such electron-hole pair is electrostatically bound and is known as the *"exciton"*. The exciton size is defined as *Exciton Bohr Radius (EBR).*

The size of a bulk semiconductor is much greater than EBR, and the excitons are confined within a large volume. Due to the presence of a large space, it requires a relatively smaller energy for the exciton confinement. On the other hand, in nano-sized quantum dots exciton needs to be confined in a small volume which is usually comparable to the material's

EBR. Confining the excitons within much small volume requires much more energy compared to bulk semiconductor. Therefore, quantum dots always have a larger band gap than their bulk analogs. The presence of fewer atoms in QDs compared to the bulk results in discretization and quantization of electron energy levels which resembles those of an atom.[1] This is why quantum dots are sometimes called as artificial atoms.

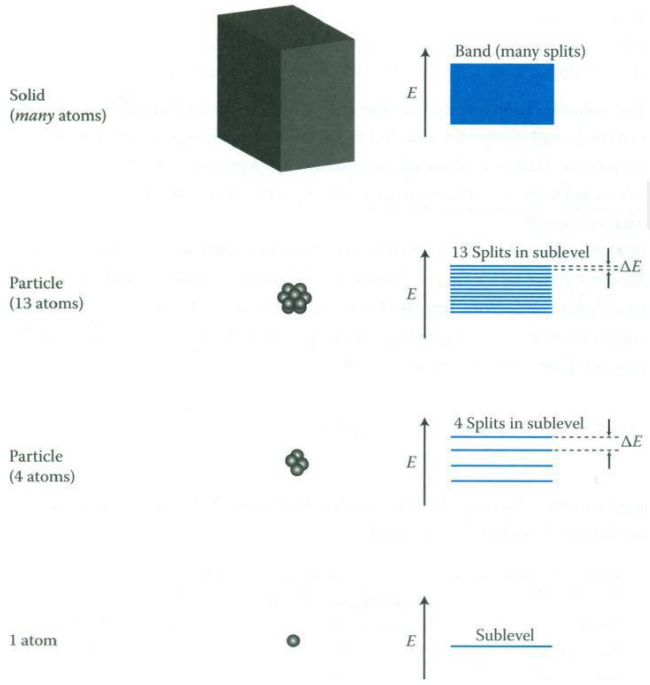

Figure 1.3 Discretization of energy levels of an atom. Few atom particles and the bulk solid [11]

Louis Brus, who discovered quantum dots in colloidal solution, modified the Schrödinger's equation to relate the particle size to the band gap energy of that QD, since band gap energy of semiconductor QDs depends on its size.[13, 14]

$$Eg_{QD} = Eg_b + \left(\frac{h^2}{8R^2}\right)\left(\frac{1}{m_e} + \frac{1}{m_h}\right) - \left(\frac{1.8e^2}{4\pi\varepsilon_0\epsilon R}\right) \quad \textbf{Equation 1.1.1}$$

In the equation 1.1, Eg_{QD} and Eg_b are the band gap energies of QD and bulk semiconductor, respectively. R is the radius of the QD, h is the Planck's constant, m_e is the effective mass of the electron in the bulk, m_h is the effective mass of the hole in the bulk, 'e' is the charge of an electron, 'and 'ε' is the dielectric constant of the bulk. According to eq. 1.1 band gap energy of the QD increases with decreasing particle size (**Figure 1.4**).

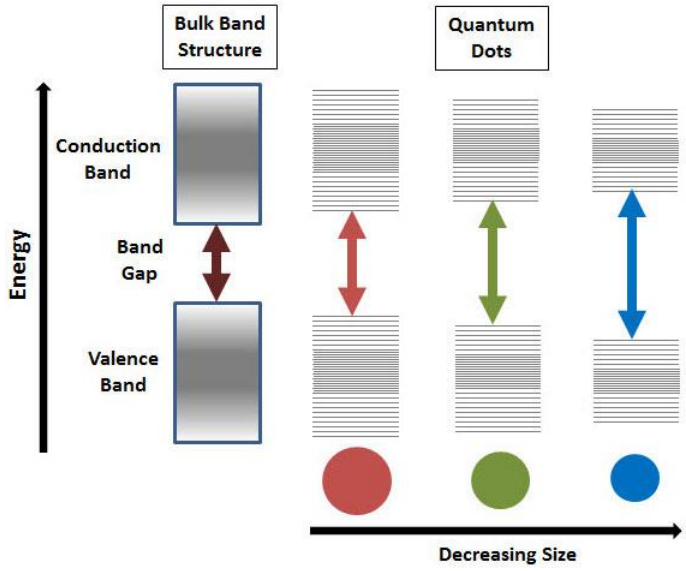

Figure 1.4 Size-dependent band gap energies of Quantum Dots [15]

1.1.2 Optical Properties of QDs

QDs can be excited by a photon with an energy equal or higher than the band gap energy resulting in the formation of electrostatically bound electron-hole pair, the process also known as absorption of light. Electrons in the excited state with excess energies are unstable and prone to return to its ground state by giving the excess energy off as a heat or photon. Excited electron relies mostly on two different pathways to relax back which strongly affect the optical properties of QDs: 1. Radiative process through electron-hole recombination, 2. Non-radiative processes trough surface trapped states located between CB and VB.[16] Excited electrons may relax via nonradiative pathways to the lowest allowed energy level in the conduction band via vibrational relaxations. During this process, electrons lose part of the absorbed energy as heat. Afterwards, electron-hole recombination may occur via a radiative process in which a photon is emitted, the phenomenon called *fluorescence*.[17] Such electron-hole recombination is also referred as band-edge emission. Due to loss of energy through non-radiative relaxations, the energy of the emitted photon shifts to a longer wavelength in comparison to the energy of the absorbed light. The difference in wavelength of emitted and absorbed photons is called as *Stoke's shift*. [18]

Since the band gap is size dependent due to the quantum confinement is nanometer scale, it is possible to tune the absorption energy for the generation of an exciton, the first excitonic peak, or the emission wavelength of QDs can be tuned with the size. As the size of QDs

increases, the band-gap energy decreases and the first excitonic peak and emission maxima shifts to longer wavelengths in the electromagnetic spectrum (**Figure 1.5**).[19]

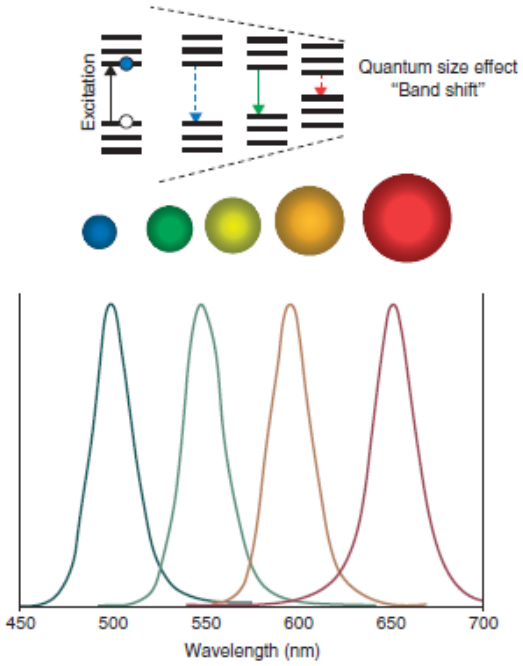

Figure 1.5 Size-tunable emission profile of QDs[19]

Alternative to the electron-hole coupling, excited electron may be trapped at defect related energy states between CB and VB which is usually a non-radiative relaxation. However, some QDs exhibit trap state emission as the sole emissive process or in addition to the band-edge emission. [20, 21] Naturally, such emissions are usually detected at a much longer wavelength than the band-edge emission (**Figure 1.6**).

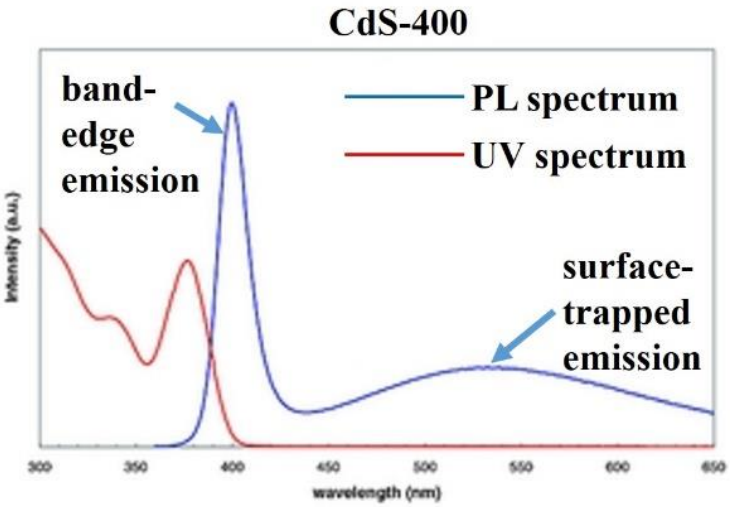

Figure 1.6 Stoke's shift, band-edge and surface-trapped emission profile of CdS QDs [22]

Large surface to volume ratio of QDs due to their very small sizes, make them prone to surface defects which dramatically change their optical properties. Such surface defects are usually dangling bonds, lattice mismatches or vacancies where the excited electron might be trapped. [23]

One approach to eliminate such surface defects and enhance band-edge emission is to grow a shell on top of the core material.[19] Core-shell nanocrystals (NCs) have gained a significant attention due to high fluorescence quantum yield (QY), large emitting range, resistance to photo-oxidation, pro-longed PL decay times and so on.[24] Core-shell NCs might be categorized under three basic types depending on the relative bandgap alignments of core and shell materials: type-I, type-II and reverse type-I (**Figure 1.7**).[12] Among these

three types of core-shell NCs, type-I systems have been developed to passivate the QD surface and improve fluorescence QY and optical stability by the overgrowth of another semiconductor material with a larger bandgap energy on top of the core material. By growing a shell around the core material, the electrons and holes are trapped inside the core which improves the fluorescence QY and other optical properties by isolating the core from the environment. Thus, the electron transfer from the type-I NCs theoretically is not allowed. The most common example of type-I NCs is CdSe-ZnS core-shell NCs.[25, 26]

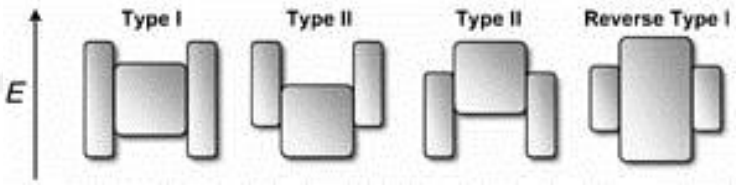

Figure 1.7 Representation of bandgap alignments of different types of core-shell NC systems.[12]

1.2 Classification of Polymerization

The first classification of polymers is made by Carothers in 1929.[27] Carothers' classification relies on the difference in the composition of the polymer and the monomer. *Condensation polymerizations* involve elimination of small molecules, typically H_2O, from

the chemical reactions of monomers, whereas *addition polymerizations* provide polymers that have the repeating units with the molecular formula identical to the monomer. Carothers' method of classification was not entirely satisfactory because some addition polymerizations exhibit the characteristics of a typical condensation polymerization or vice versa.

Later, a better terminology for the classification is provided based on the polymerization mechanism.[28] In *step-growth polymerizations*, the polymerizations proceed stepwise through reactions between two molecular species such as monomer or oligomer. In *chain-growth polymerizations*, monomers are sequentially added to the active end on the growing chain to yield the polymer. Chain and step-growth polymerizations have different features, but the most significant difference is in the character of the reacting species.[29] Step-growth polymerizations require functional monomers, while chain-growth polymerizations need an initiator molecule to start the chain growth and monomer. Another significant difference is in the molecular weight development (**Figure 1.8**).[30] Molecular weights the polymers rely on the extent of polymerization. In step growth polymerizations, molecular weight depends on the extent of the reaction and reached to high values at almost full monomer conversions. On the other hand, molecular weight of the polymer chains are fixed early in the reaction in chain-growth polymerizations.

Chain-growth polymerizations require an initiating specie to attack a monomer to start the chain growth. The initiating molecule determines the mechanism of the

polymerization. In chain-growth polymerizations, initiating specie can be a radical, anion or cation.[29] Although free radical, anionic and cationic initiators are able to initiate chain-growth polymerizations, they cannot be utilized in all kinds of monomers. Ionic initiators are highly monomer selective which limits their use. Radical initiators are the mostly widely used ones in polymerization of vinyl monomers. Many industrial processes involve free radical polymerization of vinyl monomers, as well.

All chain-growth polymerizations essentially contain three fundamental steps: initiation, propagation and termination.[31] Those three steps will be explained in detail in the context of free radical polymerization.

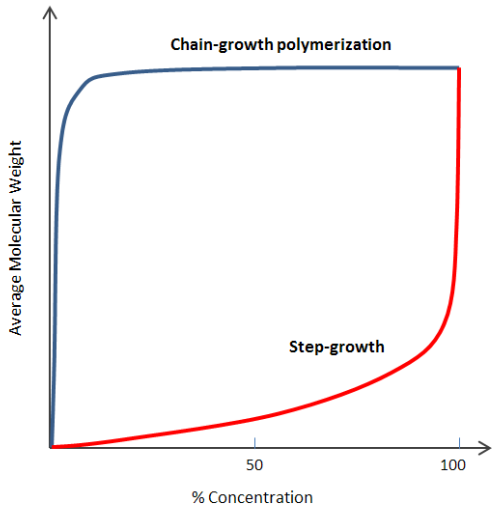

Figure 1.8 Chain vs Step Growth Polymerization[30]

1.2.1 Mechanism of Free Radical Polymerization

Free radicals are highly reactive species with an unpaired electron that usually exhibit short lifetimes.[31] The carbon-centered free radicals have sp2 hybridization and are highly reactive towards the double bonds of unsaturated monomers (**Scheme 1.1**). The first studies investigating the mechanism of free radical polymerization were performed by Flory in 1939.[32] Free radical polymerization have become the most commonly practiced polymerization for vinyl monomers since the first studies of Flory because most of the monomers are prone to this type of chain polymerization.[31] Like other types of chain-growth polymerizations, free radical polymerizations have typically three basic steps which are initiation, propagation and termination. , "Chain transfer" may be considered as a fourth step.

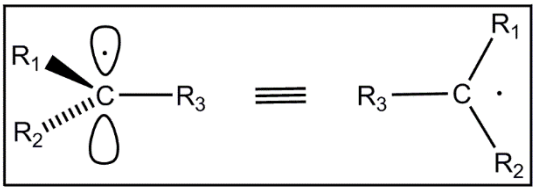

Scheme 1.1 Representation of general structure of a carbon-based free radical[31]

1.2.1.1 Initiation

The first step of free radical polymerization is the initiation. This step consists of two distinct reactions. In the first reaction, free radicals are generated from an initiator molecule by homolytic cleavage of labile bonds (i.e. peroxides –O–O– or azo –N=N–) or by a redox

reaction. In the subsequent reaction, this free radical reacts with electrons found in the *p* orbitals of carbon-carbon double bond of the unsaturated monomer to form the monomeric free radical or chain initiating radical called as active center.

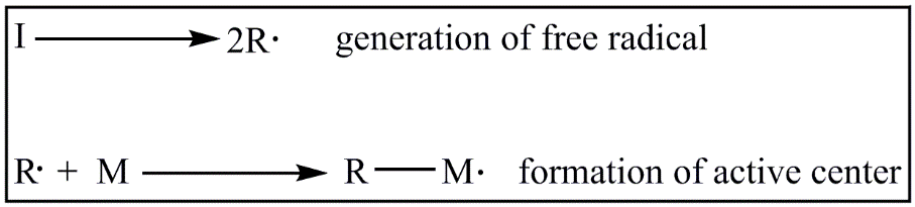

Scheme 1.2 *Formation of initiating specie and active center in the initiation step*

Homolysis of the initiator molecule may be induced by heat (thermolysis) or radiation (photolysis). Photolysis is very advantages since it can be performed at room temperature and can provide an on/off switchable reaction. Advantages and disadvantages of photoinitiated free radical polymerizations and types of photoinitiators will be explained later in detail.

1.2.1.2 Propagation

Active centers rapidly adds monomers to the growing chain and after each subsequent addition a new active center forms at the end of the growing chain.

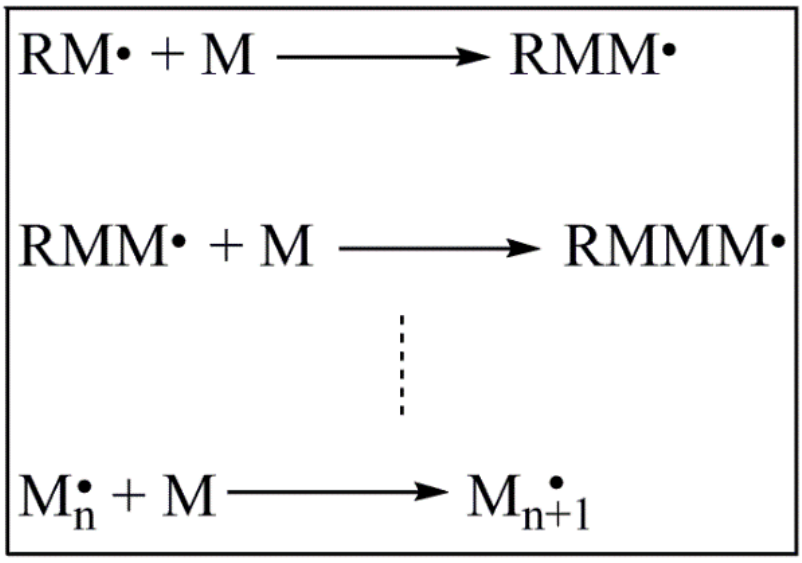

Scheme 1.3 Typical propagation reactions of free radical polymerization

1.2.1.3 Termination

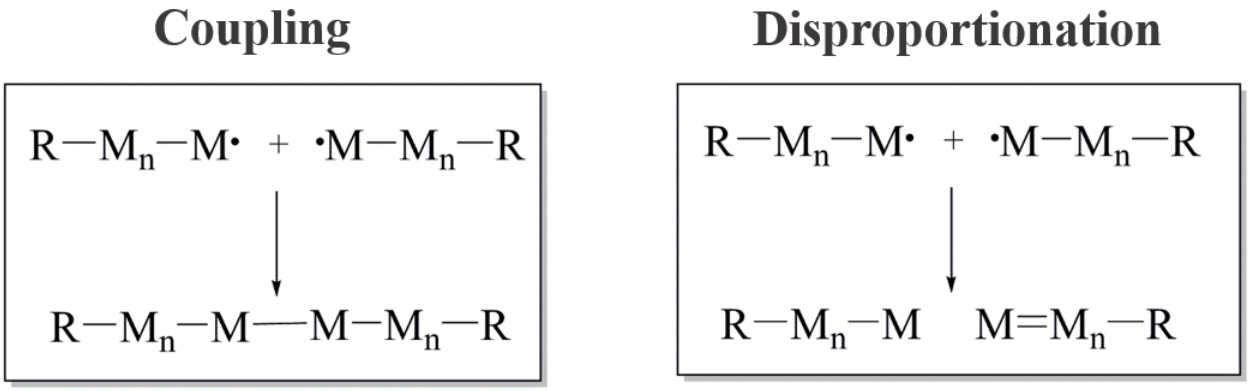

Scheme 1.4 Termination by coupling and disproportionation

In the termination step, the bimolecular reaction of two radicals occurs to give a dead polymer, meaning that propagation of active chains ceases. Typically two mechanisms dominate the termination step. (**Scheme 1.4**) *Coupling* is the process by which two growing chains combine to give a polymer with the initiator fragment at the ends of the polymer. Another process is *disproportionation*. In disproportionation mechanism, a hydrogen atom on the beta carbon of one growing chain is abstracted by another growing chain. This process results in a polymer with an unsaturated end group at one end plus a polymer with a saturated end.

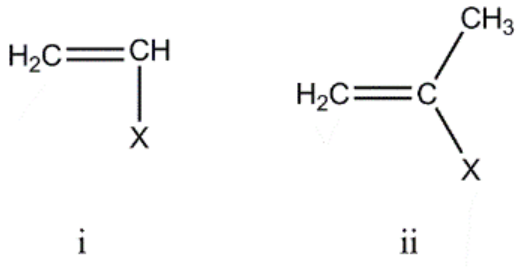

Scheme 1.5 *(i) vinyl monomers, (ii) alpha-methyl vinyl monomers*

Combination process usually takes place with the vinyl monomers (i) while disproportionation occurs typically with alpha-methyl vinyl monomers (ii). Typical examples of combination and disproportionation are termination of styrene polymerization and methyl methacrylate polymerization, respectively. Coupling process usually takes place with the vinyl monomers (i) while disproportionation occurs typically with alpha-methyl

vinyl monomers (ii). Typical examples of combination and disproportionation are termination of styrene polymerization[33] and methyl methacrylate polymerization[34], respectively.

1.2.2 Photoinitiated Polymerizations

Light-mediated polymerization, commonly recognized as photopolymerization, has gained remarkable attention due to its several advantages over thermal or redox polymerizations in last three decades.[35, 36] Two widely studied routes are free radical and cationic photopolymerizations. Occasionally examples of anionic photopolymerizations are reported in the literature.[37-39] Although cationic polymerization offers some advantages over free radial route such as no inhibition by O_2 molecule, variety of monomers with different functionality plus to monomers containing olefinic double bonds, photoinduced free radical polymerization is still the most preferred one in the industrial applications.[35] Photoinduced free radical polymerization has become a practical method utilized in many important processes of everyday life in a variety of applications including dentistry[40], adhesives[41], coatings[42], 3-D fabrication of objects[43], inks[44], optical waveguides[45], etc..

In photopolymerizations, the driving force behind the radical formation is the electromagnetic radiation, usually UV light and visible light as the energy source. This initiation route can be performed at room temperature or at much lower temperatures

compared to thermally initiated polymerizations. This is a tremendous advantage in case of temperature sensitive applications such as dentistry, bone cement, etc. and also for curing of large species such as films, coating etc. .

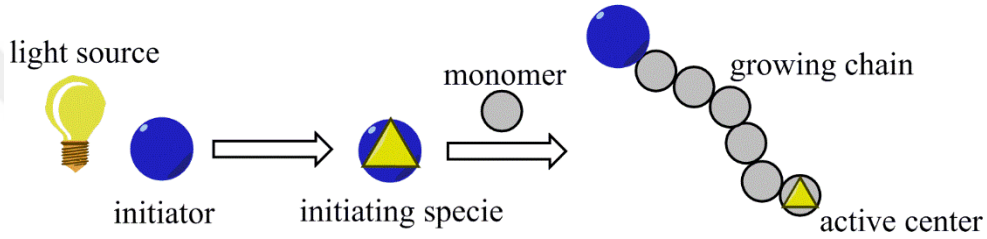

Scheme 1.6 A general flow of photopolymerization process[35]

Another highly desired property of photopolymerization technique is the control of polymerization by simply turning the light on/off since the reactive species form immediately when light is on and disappear when light is off. Moreover, photopolymerization provides fast curing in a more energy efficient way with much less waste (i.e. solvents) and provides spatial and temporal control of polymerization. In addition to so many advantages, it has couple of disadvantages as well. The cure depth is the major one. Usually UV light is used for the fast curing of many monomers, but the penetration depth of UV light is limited to few millimeters. This prevents curing of thick species. Besides, high energy UV light is not safe.

As shown in **Scheme 1.6**, photopolymerization starts with the irradiation of light which is absorbed by the photoinitiators. Upon irradiation, the initiator molecules get excited

into the triplet state and then immediately generate free radicals with two different process: a-cleavage or H-abstraction. Based on these two processes, photoinitiators are classified into two groups: type-I and type-II photoinitiators.

Type-I photoinitiators are also known as unimolecular photoinitiators and are one-component photoinitiating systems[46]. When irradiated, usually in the UV, type-I photoinitiators are excited to triplet state and rapidly undergoes alpha bond-cleavage, generating two free radicals (**Figure 1.9**). Typical examples are benzoin and its derivatives, benzyl ketals and alkyl-phenones with appropriate substitutions.[47]

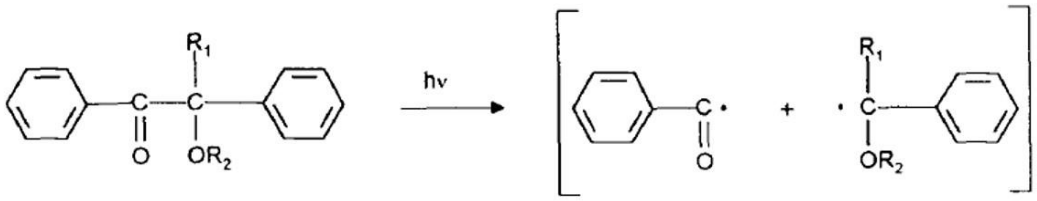

Figure 1.9 Typical representation of **b**enzoin derivatives as type-I PIs[47]

Type-II photoinitiators are two component systems: photoinitiator and a co-initiator (hydrogen donor).[47] Upon irradiation at appropriate wavelength, the initiator gets excited to triplet state and then interacts with the co-initiator molecule by an electron transfer or hydrogen abstraction. The proposed mechanism suggests that an electron is transferred from the co-initiator to excited triplet state of the initiator molecule forming a new "initiator – co-

initiator complex" and the H-abstraction from the alpha carbon of the co-initiator takes place which results in the formation of two free radicals.[48] So, the reactive initiating radical forms from the co-initiator via biomolecular H-abstraction. However, the radical formed on the initiator molecule generally do not act as an initiator due to the steric hindrance and delocalization of the free electron.[35] Most widely used type-II photoinitiators are benzophenones and thioxanthones (TX) (**Figure 1.10**).[47, 49] Co-initiators can be amines, alcohols, ethers and thiols. Among the co-initiators, tertiary amines such as triethyl amine (TEA) are the most studied ones which is prone to donate H-atom from the alpha position of N atom. **Figure 1.11** illustrates the initiation mechanism of iron-oxide initiated photopolymerization in the presence of TEA as a co-initiator.[50]

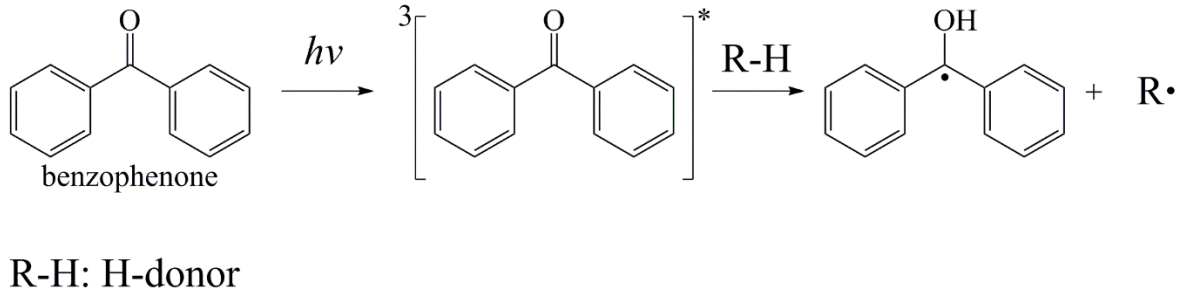

Figure 1.10 A general process for the formation of the initiating specie using benzophenone as a type-II PI

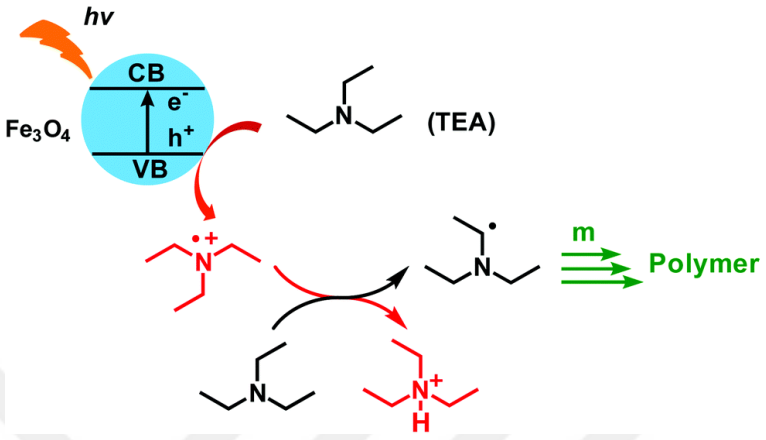

Figure 1.11 The initiation mechanism of iron-oxide initiated photopolymerization with TEA as a co-initiator[50]

Type-II photoinitiators usually show a slower rate of curing in comparison to type-I photoinitiators since the initiation requires a biomolecular reaction. But these types of photoinitiators have recently gained lots of interest because they are capable of absorbing light in the visible region when they are modified with appropriate substituents (i.e. carbazole functionalized thioxanthones, amine conjugated thioxanthones derivatives).[51, 52] Initiation in the visible region improves the penetration depth and safety of the irradiation.

In general, photoinitiators do absorb light at a very narrow wavelength range, usually in the high energy UV region. This pose a safety issue, limited penetration depth for cure and may be unreacted species. Upon irradiation two free radical species form and only one of them initiates the polymerization. This again provides small, unreacted species which migrate to surface causing toxicity, odor and coloring.

Lately, one component type II photoinitiators which can be activated in the visible region has emerged.[53, 54] TX molecules have been modified to in such a way that they become able to initiate the polymerization in the absence of a co-initiators. TX moieties conjugated with the anthracene[53] or bound to multiple aromatic groups[55] containing molecules have been reported as one-component type-II visible light activated initiators (**Figure 1.12**).

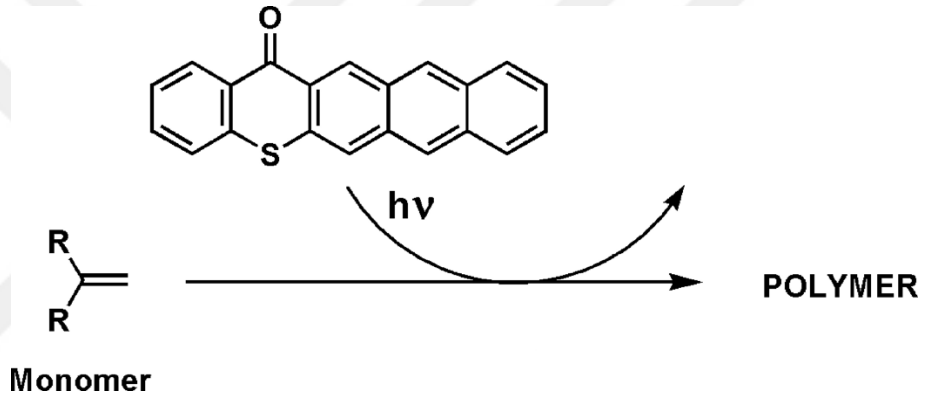

Figure 1.12 Thioxanthone-anthracene as one-component type-II PI in FRP[53]

1.3 Quantum Dots as Photoinitiators in Literature

A promising alternative to the organic photoinitiators is photoresponsive QDs.

Compared to organic molecules, QDs have a very broad and continuous absorbance band usually extending into or beyond the visible region and a large extinction coefficient which would be very practical for photoinitiation process.

The first example to the utilization of semiconductor NPs in the photopolymerization was reported by Oster *et al.* in 1966 wherein bare zinc oxide sensitized polymerization of vinyl

monomers was performed in an aqueous media.[56] Hoffmann *et al.* utilized small, uncoated nanoparticles, ZnO[57] and CdS[58], as a PI in the methyl methacrylate (MMA) photopolymerization in alcoholic solvents. They have claimed three important features for this polymerization: 1. Using nano-sized particles reduces light scattering, hence increases initiation efficiency. 2. Initiation starts with an anionic but continues with a radical mechanism. 3. Hole-scavenging solvents are necessary for the process, and isopropanol and ethylene glycol were the best for ZnO and CdS initiated photopolymerizations, respectively. In these studies, precipitation polymerization was performed and no luminescent nanocomposites were reported.

Strandwitz *et al.* performed a more detailed study on photopolymerization of MMA using a colloidal QD (oleic acid coated CdS, band gap 3 eV, size 3.7 nm, emission peaks at 410 and 600 nm) for the first time.[59] They have not seen an effective polymerization without TEA, but bulk polymerization with TEA provided 11 % conversion in 120 min. They have suggested electron transfer from amine to the conduction band hole since, successful polymerizations resulted in luminescence quenching. In these studies and the few others on this matter, production of the nanocomposite was not intended, but instead QDs were utilized just as a PI and removed from the final polymer.

Yet, Zhang *et al.* produced composite hydrogels from the photopolymerization of poly(*N*,*N*-dimethylacrylamide)/clay/nanoparticle (NP) mixture using several different

NPs.[60] Thioglycolic acid coated CdTe QDs retained their luminescence after the polymerization. This group was the first one who utilized the QDs as a PI to produce a nanocomposite and demonstrated maintenance of the QD luminescence. These polymerizations were performed in water and hydroxyl radical and monomer radical generated upon photoexcitation of QDs are suggested as the initiating species.

These examples indicate the major approaches, progress and therefore the milestones in evaluation of NPs as PIs. It is clear to us that the photoinitiation is getting better with colloidal particles but the mechanism is not clear yet and the destiny of the particles after successful polymerization is being debated. Also, this literature clearly shows that only recently, presence of the NP initiator in the final polymer is valued, since the knowledge of NPs advanced dramatically.

1.4 Research Proposal

Photopolymerization of acrylics is widely used in the production of many current and emerging materials for dental/medical use, paints, coatings, inks, adhesives, masks, plastics, etc. In addition to such commercial products there are some niche applications such as coating nanoparticles and cells with hydrogels utilizing photo-curing reactions. Most of these applications actually utilizes the technique for curing reactions where crosslinked polymers are formed in place. Major advantages of the technique, which usually utilizes UV excitation of an organic dye, is the room temperature polymerization and suitability to many different

vinyl monomers. Nanoparticles are an ingredient in many cured polymeric material for various reasons such as mechanical strength, superhydrophobicity and functionality (magnetic, luminescent, catalytic, etc.). Vice versa, polymeric materials may provide stability to NPs. Combination of polymer/NP composites are not trivial actually. Yet, there seems to be an unexploited venue for the synthesis of such composite structures. Use of NPs as photoinitiators in radical polymerization/curing of vinyl monomers producing nanocomposites. There are very few studies reporting NP based Photoinitiators (NPI) but the mechanism and the effect of photopolymerization on particle properties are debatable. There are only few reports studying good quality colloidal quantum dots as a PI and only one which reports a crosslinked composite nanomaterial.

This thesis project aims to investigate colloidal QDs with luminescence in the visible region as PIs in the free radical photopolymerization of acrylates and methacrylates with the following purposes:

1. Understand the initiation mechanism,
2. Produce nanocomposites in a simple one step process,
3. Provide colloidal QD/polymer structures,
4. Evaluate their potential as long-wavelength initiators.

Today, how and why QDs act as a PI and which properties influence the PI efficiency is not completely clear. Therefore, the influence of the QD composition, size, surface quality

and surface composition on PI efficiency is studied in this thesis work. Influence of the photopolymerization on the luminescence properties of QDs is also investigated.

Since until now, photopolymerization reactions utilizing QD PIs were performed in alcohol or water and hence hole-scavenging role of the solvent and hydroxyl or alkoxy radicals were suggested as possible initiating species, in order to identify the role of QDs better, only hydrophobicly modified QDs and toluene was used as a solvent in this study.

As a PI colloidally stable, organic soluble, luminescent CdX QDs (X = S, Se) in different size with different coatings were synthesized for the study.

In the first part, oleic acid coated CdS QDs with different crystal size and quality was evaluated as a photoinitiator in batch photopolymerization of MMA. Kinetics of photopolymerization was discussed based on the photo-DSC studies performed with PEGDA and HDDA as monomers. Also, studies directed towards the identification of the initiating specie were summarized in this part. In the second part, impact of core-shell structure on the photoinitiation process is discussed based on the studies performed with CdSe-ODA and CdSe-ZnS-ODA QDs.

2. Experimental

2.1 Materials

Cadmium acetate dehydrate, $Cd(CH_3COO)_2.2H_2O$ and oleic acid (technical grade, 90%) were purchased from Merck. Thioacetamide, octadecylamine (technical grade, 90%), 1-octadecene (technical grade, 90%), absolute ethanol, acetone, methanol and toluene were purchased from Sigma-Aldrich. Methyl methacrylate (MMA, 99%; Merck), poly(ethylene glycol) diacrylate (PEGDA, M_n = 575 $gmol^{-1}$; Sigma-Aldrich) monomers and 1,6-Hexanediol diacrylate (technical grade, 80%; Aldrich)were purified through a basic Al_2O_3 column to remove inhibitor.

Octadecylamine (ODA) stabilized CdSe QDs and CdSe-ZnS core-shell QDs were purchased from NNCrystal and used in photopolymerization studies.

2.2 Synthesis of Oleic Acid Stabilized CdS QDs

Cadmium acetate dehydrate (53.3 mg), oleic acid (4.0 mL) and 1-octadecene (20.0 mL) were added into a round bottomed flask. The flask was placed into a hot oil-bath at 140 ^oC and the mixture was stirred vigorously for 30 minutes under argon flow. Then, thioacetamide

(15.0 mg) was directly added to the reaction mixture and the reaction was allowed to continue for 10 minutes. Reaction was quenched by cooling to room temperature in a cold-water bath. CdS-OA QDs were precipitated in an excess ethanol-acetone mixture, separated with centrifugation, vacuum-dried and redispersed in toluene.

2.3 Synthesis of CdS-OA in Different Crystal Sizes

2.3.1 Synthesis of CdS360

Cadmium acetate dehydrate (53.3 mg), oleic acid (1.0 mL) and 1-octadecene (10.0 mL) were added into a round bottomed flask that was placed into an electronic heating mantle. The flask was heated to 140 ºC and the mixture was stirred for 30 minutes under Argon flow. TAA (15.0 mg) as a sulfur source was directly added to the reaction flask. The reaction was stopped at 1 minute by quenching it to room temperature in a cold-water bath. QDs were first precipitated with excess acetone to remove 1-ODE, redispersed in toluene and then re-precipitated with excess methanol to remove the excess oleic acid. After the vacuum-drying, QDs dissolved in toluene were ready for the further use. QDs were labeled as **CdS360** and stored at 4 ºC in the dark.

2.3.2 Synthesis of CdS400

It was almost the same procedure with two modifications. Oleic acid amount and the reaction duration increased from 1.0 mL to 4.0 mL and from 1 min to 30 min, respectively. The same purification steps were followed. The QDs were labeled as **CdS400.**

2.4 Batch Polymerizations

In all batch polymerizations, 2.0 mL toluene and 2.0 g MMA were used along with the desired amount of QD. After argon purge, polymerization mixtures were irradiated at 365 nm in a Rayonet equipped with 18 lamps (Philips 8W BLB, 365 nm, 22 mW/cm^2). All samples were precipitated in a cold methanol and dried under vacuum. The given QD wt% and TEA wt% values were calculated according to 2.0 g of monomer.

2.5 Kinetic Studies by Photo-DSC

TA Q100 DSC equipped with Omnicure 2000S and two different emission filters allowing light between 320-480 nm and 400-500 nm were used. Typically, a 5 mg/mL QD solution in toluene was prepared for Photo-DSC studies as an initiator solution. To prepare the polymerization mixture, 200 µL QD solution was added into 0.2 g monomer and stirred for a few minutes to disperse QDs. As a control, 0.2 g monomer mixed with 200 µL toluene was used. A 10 µL portion of these polymerization mixtures was transferred into a photoDSC pan. After 5 min nitrogen purge the sample was irradiated at the desired a light intensity (30 to 50 mW/cm^2) in an isothermal mode at 30 ^oC. Separate reactions were performed for different excitation filters. After irradiation, samples were kept in dark for 1 minute. The rate of polymerization (R_p) was calculated from the heat released from the double bond conversion according to the following formula:

$$Rp = Q_t/n \times E_{db}$$ **Equation 2.1**

Where Q_t (J mol^{-1} s^{-1}) is the amount of heat that is released at time t, n is the number of acrylate double bonds and E_{db} is the energy of the double bond (for acrylates 86 kJ mol^{-1} for methacrylates 54.4 kJ mol^{-1}).[61, 62]

2.6 Characterization and Instrumentation

UV-vis spectra were recorded using Schimadzu UV-Vis-NIR spectroscopy. Photoluminescence measurements were recorded by HORIBA JOBIN YVON Fluoromax-3. Photoluminescence spectra of QDs were performed at the excitation wavelength of 355 nm with entrance and exit slit widths of 5.0 nm. Absolute photoluminescence quantum yield measurements were recorded by Horiba Fluorolog 3 spectrofluorometer equipped with integrating sphere. The optical density of the QDs was around 0.1 at their excitation wavelength of 365 nm. Transmission electron microscopy (TEM) images were taken by Tecnai G2 F30 at bright field high resolution (HR) TEM (acceleration voltage 200 kV) using samples deposited on carbon coated Cu-grid from dilute solutions.

Molecular weights of the PMMA samples freed from QDs were determined with gel permeation chromatography (GPC) (Agilent 1100) equipped with a refractive index detector, Polymer Labs PLgel 5µm Mixed-C column working with THF eluent at a flow rate of 1.0 mL/min at 30 °C. In order to remove QDs from the polymers, PMMA/QD samples were dissolved in THF and treated with 10% HF solution overnight followed by precipitation in

methanol. To ensure complete removal of QDs, the process was repeated twice and the final polymer was dried under vacuum. QD free polymers were dissolved in THF and passed through a 0.20 µm syringe filter. Molecular weights were estimated based on the calibration curve created with Polystyrene standards in the molecular weight range of 580 to 1.12×10^6 Da.

T_g analysis of polymers and PMMA/QD composites were carried out with TA Differential Scanning Calorimetry Q200 in the temperature range of 10-160 ºC at a heating rate of 10 ºC min^{-1} under N_2 gas flow. T_g values were calculated from cycle 2.

Dynamic light scattering (DLS) measurements were performed with Malvern Zetasizer Nano ZS at room temperature.

Functional groups were investigated using the dried samples and Thermo Scientific Nicolet iS10 ATR-IR.

ESR-ST experiments were carried out using an X-Band spectrometer (EMXplus Bruker). The radicals were generated at room temperature through light irradiation with a LED@365 nm (Thorlabs M365L2, 190 mW) in a nitrogen saturated tert-butylbenzene solution. The light generated radicals were then trapped by phenyl-N-tertbutylnitrone (PBN) as a spin trap agent according to a procedure described in detail elsewhere.[63-65] The acquisition parameters were 1.10^5 for the receiver gain, 1 G for the modulation amplitude, 20.48 ms for the tis constant and 6.325 mW (15 dB) for the power. Spectra were accumulated over 10

scans. Finally, the ESR spectra were simulated using WINSIM (a NIEHS Public EPR Software Tool). [66]

3. Evaluation of Quantum Dots as Photoinitiators in Free Radical Polymerization of Vinyl Monomers

3.1 Synthesis and Characterization of Oleic Acid Stabilized CdS QDs

Yellow luminescent oleic acid coated CdS QDs were prepared in 1-octadecene from cadmium salt and thioacetamide. These particles (QY 71%, size 2.96 nm) have first excitonic peak at 380 nm and emission maxima at 420 and 584 nm corresponding to band-edge and trap state emissions, similar to commercial or previously reported CdS-OA of similar size (**Figure 3.1**). These particles can be easily suspended in toluene after purification.

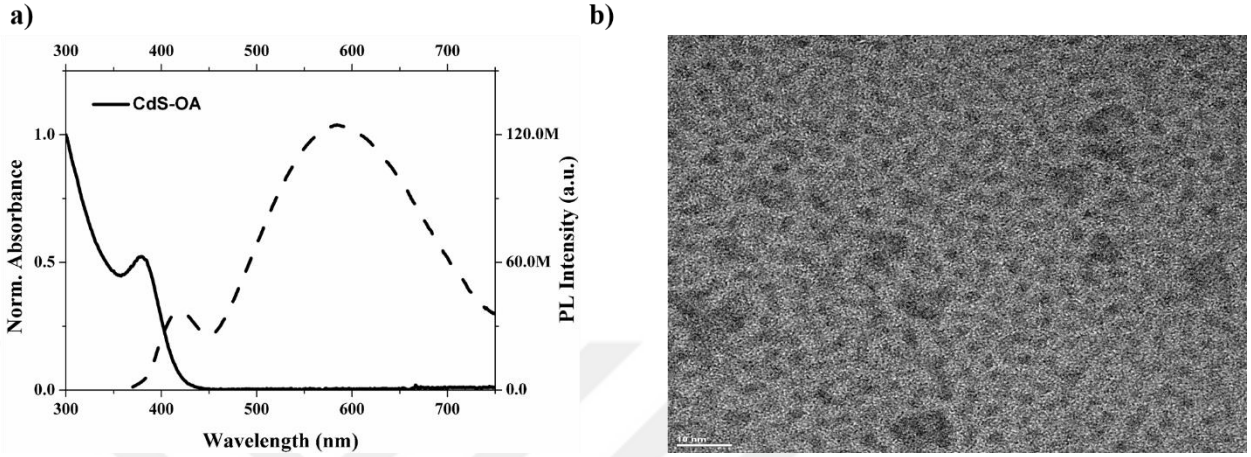

Figure 3.1 a) UV-PL spectra of CdS-OA and b) TEM image at the scale bar of 10 nm

3.2 Evaluation of CdS-OA as a photoinitiator in the FRP of MMA

Purified CdS-OA QDs were evaluated as photoinitiators in photopolymerization of acrylic monomers in a non-aqueous medium. Before starting QD initiated MMA polymerizations, several control experiments were carried out to ensure that QDs play significant role in the initiation of polymerization. In the absence of light, QD-MMA solution did not polymerize. When QD was absent in the polymerization solution, no observable polymer till 7 h illumination was produced. Since CdS-OA QDs were stabilized by oleic acid (OA), it may play a role as an ingredient of polymerization solution. However, oleic acid itself could not initiate the polymerization of MMA. So, control experiments proved that CdS-OA can initiate polymerization of MMA only when the mixture containing CdS-OA QDs is irradiated (**Table 3.1**).

Table 3.1 Control experiments of methyl methacrylate polymerization*

ID	Initiator	Light	Time [h]	Conv. [%]
Control 1[a)]	QD	-	2	-
Control 2	-	+	2	-
Control 3	-	+	7	-
Control 4[b)]	OA	+	5	-
Control 5[c)]	TEA	+	2	4
Control 6[d)]	QD + TEA	+	2	17

* In all control experiments, 2.0 mL of toluene and 2.0 gram of MMA were used and experiments were performed in Rayonet.

a) 0.5 wt% CdS-OA as photoinitiator.

b) Oleic acid itself as photoinitiator.

c) 37.6 µL TEA as photoinitiator

d) 0.5 wt% CdS-OA and 37.6 µL TEA as co-initiator

Table 3.2 Polymerization of methyl methacrylate in toluene using oleic acid coated CdS QDs*

ID	QD [wt%]	Time [min]	Conv. a) [%]	T_g [°C]		M_n c) [g mol^{-1}]	M_w / M_n c)
				CdS/PMMA	PMMA b		
P1	0.2	30	0.19	-	-	-	-
P2	0.2	60	5.1	78	113	-	-
P3	0.2	120	9.49	82	115	63.3	1.543
P4	0.2	240	16.2	74	116	65.9	1.538
P5	0.1	120	0.65	-	-	-	-
P6	0.5	120	12.15	96	102	61.3	1.537
P7	0.7	120	6.32	-	-	43.8	1.434
P8	1.0	120	2.68	70	119	46.6	1.494

* Reaction solution: 2.0 mL toluene with QD and 2.0 g MMA; λ_{exc} = 365 nm.

a) Conversions were measured gravimetrically.

b) CdS-OA QDs were removed from the polymer samples.

c) Number average molecular weight (M_n) and polydispersity index were determined by GPC and M_n values were reported as M_n 10^{-3}.

Initially, MMA polymerization was studied with different amounts of the QD and at different irradiation times at 360 nm (**Table 3.2**). In 2 h polymerizations initiated with 0.1 to 1 wt% QD, monomer conversions increased with the increasing QD concentration up to 0.5 wt% reaching to 12.15 % MMA conversion and then dropped down to 2.68% at the

highest QD concentration. Since QDs were well dispersed in the polymerization mixture, this may not be due to precipitation of QDs at high concentration, but may be due to light scattering or reabsorption processes. At fixed QD concentration of 0.2 wt%, monomer conversion increased from less than 1 % to 16% when reaction time was extended from 30 min to 4 h.

T_g of CdS-OA/PMMA and PMMA freed from QDs were also determined (***Table 3.2***). All PMMA samples have a T_g value between 102-119 °C, more or less typical for PMMA. On the other hand, QD/PMMA samples had lower T_g values (70-96 °C). If the polymer chains would strongly bind to QD surface from multiple points or would be quite short that such QD-polymer interaction would reduce the chain mobility significantly, one would expect a higher T_g value than the free PMMA or two T_g values for the bound and the non-interacting portion. Indeed, molecular weight of PMMA freed from QDs were in the range of 40-65 kDa, which eliminated the possibility of short chains, and indicated that all polymers have higher molecular weight than the critical entanglement molecular weight. So, a single T_g of the QD/PMMA at lower values compared to free PMMA suggests that quantum dots are distributed homogenously across the whole polymer and increase the free volume.

One very important point to highlight here is that, all polymers had a homogeneous distribution of QDs within the polymer and all QD/PMMA samples have a strong yellow luminescence when excited at 360 nm as the initiating CdS-OA (**Figure 3.2a**). This strongly

suggests that efficient initiation by QDs do not necessarily require luminescence quenching as suggest by the prior art. Absorbance and photoluminescence spectrum of all QD/PMMA samples showed the typical first excitonic peak of CdS-OA and a strong emission peak (**Figure 3.2b, c**) with a slight shift to lower wavelengths except P8. Interestingly, the intensity of the first emission peak at 420 nm increased while the intensity of the second emission peak 584 nm decreased after photopolymerization, except for P4 and P8. The first peak is usually attributed to the band edge and the second to the trap state emissions. This suggests a change especially on the QD surface which influences the emission mechanism of QDs.

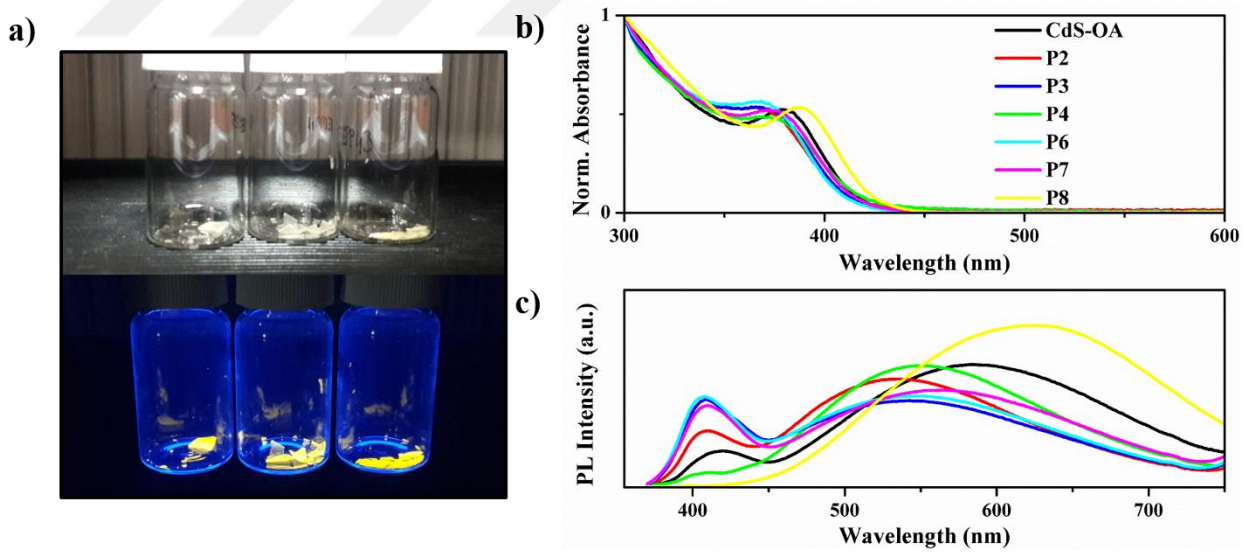

Figure 3.2 a) Luminescence of QD/PMMA under UV light (360 nm). b) Absorbance and c) PL spectra of native CdS-OA QDs and QD/PMMA samples.

When native QDs were exposed to UV irradiation under the same conditions, absorbance peak was shifted to a longer wavelength (from 380 nm to 417 nm) with some scattering at longer wavelength tail (**Figure 3.3a**). During the irradiation some precipitation occurred which would explain such behavior. Parallel to this, the emission maxima showed a red shift (from 570 nm to 609 nm) with a significant loss in the emission intensity (**Figure 3.3b**).

The results in **Figure 3.3** including loss in the PL intensity, scattering at longer wavelength and precipitation of QDs was furthermore supported by FT-IR measurements. Oleic acid molecules stabilizing QD surface were bounded to the QD surface since there was no peak that can be attributed to the free carbonyl groups that usually appear at 1750 cm^{-1} (**Figure 3.4**). However, after UV irradiation of CdS-OA QDs, a peak at ~1750 cm^{-1} appeared in FT-IR spectrum indicating the presence of unbound oleic acid molecules. The removal of coating molecule from the surface will of course lead to precipitation of QDs, and in turn decrease in the PL intensity.

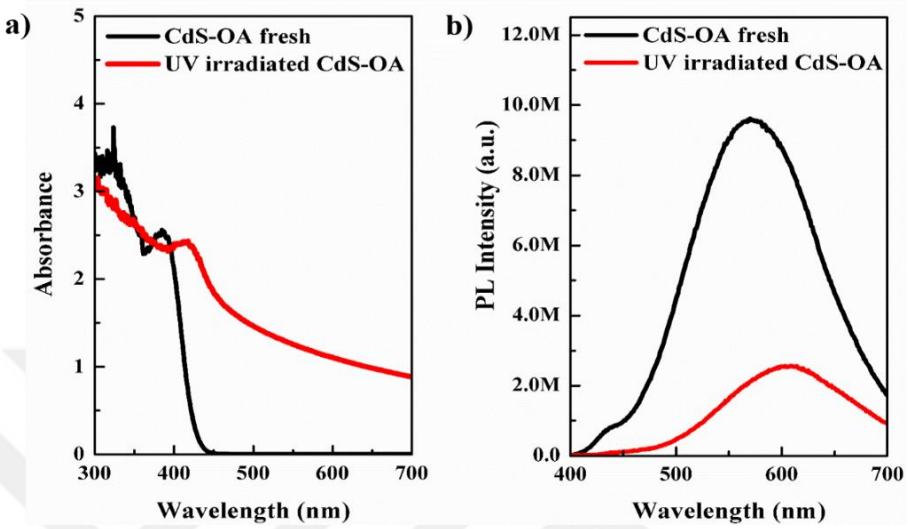

Figure 3.3 a) Absorbance and b) PL spectra of fresh and UV irradiated of CdS-OA nanoparticles in toluene.

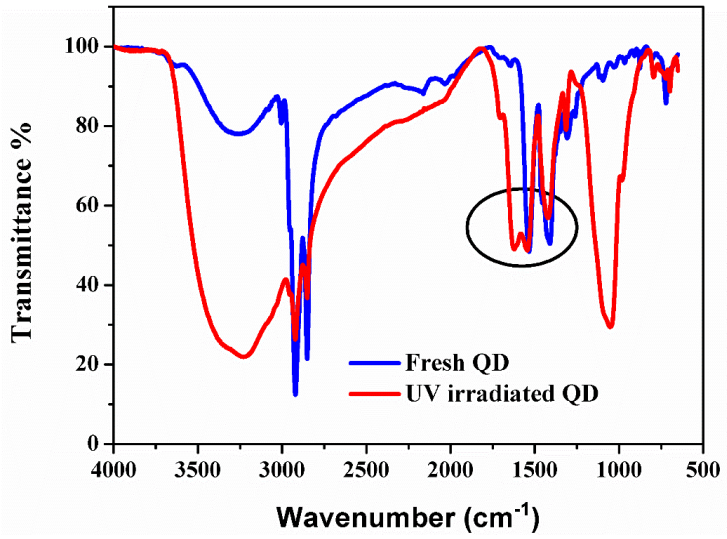

Figure 3.4 FTIR spectra of fresh CdS-OA and UV irradiated CdS-OA

Yet, photopolymerization did not cause such dramatic changes in the optical properties of the CdS-OA. Hence, these suggest that during the photopolymerization, QDs start to interact with the forming polymer providing a core-shell structure which is improving the photostability and colloidal stability. Stability is actually very critical and highly desired for practical applications of QDs or QD containing materials. Based on the DLS measurements QDs and QD/PMMA particles have about 20 and 28 nm hydrodynamic size, respectively, with much less deviation in the later, supporting improved colloidal stability (**Figure 3.5**). Based on this, it is evident that photopolymerization process causes some alterations on the surface of the CdS crystal enhancing the bandgap emission while removing emissive surface defects and providing colloidal and photostability.

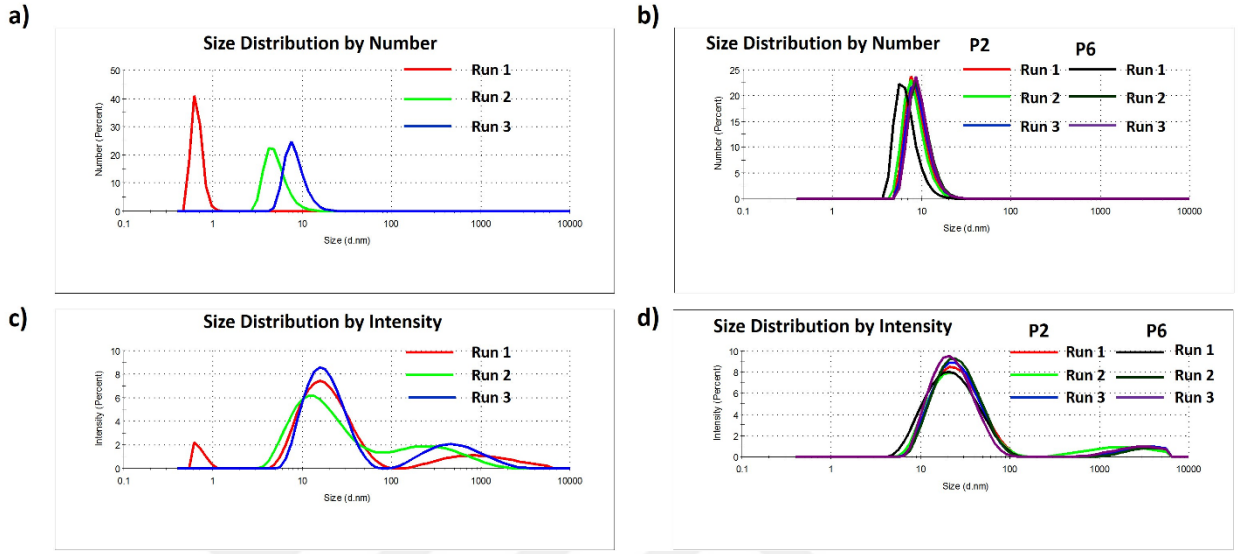

Figure 3.5 DLS measurements of CdS-OA QDs, P2 and P6 samples in toluene. a) CdS-OA QDs; size distribution by number, b) P2 and P6 samples; size distribution by number, c) CdS-OA in toluene; Size measurement by intensity, d) P2 and P6 samples; size distribution by intensity

3.3. Kinetics of the photopolymerizations initiated with CdS-OA

Kinetics of the photopolymerization was studied by means of photo-DSC. Since QDs have a continuous absorbance in a relatively broad range and these CdS-OA QDs absorb until around 450 nm, we have used two different excitation filters in order to evaluate these QDs` potential as a long wavelength initiator: a 320-480 nm filter covering a large window from UV into the visible and a 400-500 nm filter which is a safer long wavelength range. For the photo-DSC studies PEGDA was used. **Figure 3.6** illustrates the rate of

polymerization and monomer conversion with time for the PEGDA polymerizations using 0.5 wt% QD and irradiation power of 50 mW cm^{-2} using these filters. About 85 and 40% monomer conversions were achieved in 5 min using 320-480 nm and 400-500 nm filters, respectively (**Figure 3.6a**). These values can be improved significantly if polymerizations would be carried out for 15 min. (**Figure 3.6b**). However, although much slower, PEGDA shows a significant autopolymerization (63% conversion) at this irradiation power in 15 min if 320-480 nm filter is used (**Figure 3.6c**). On the other hand, PEGDA does not autopolymerize at all if the long wavelength filter is used. PEGDA conversion reaches to about 85% in 15 min using 400-500 nm filter, proving CdS-OA QDs as a very effective new long-wavelength initiators. In addition to PEGDA monomer, photopolymerization kinetics and conversion of HHDA were also studied. About 30% HDDA conversion using 0.5 wt% CdS-OA was achieved with 320-480 nm filter (**Figure 3.7**). However, it did not give polymerization with 400-500 nm filter.

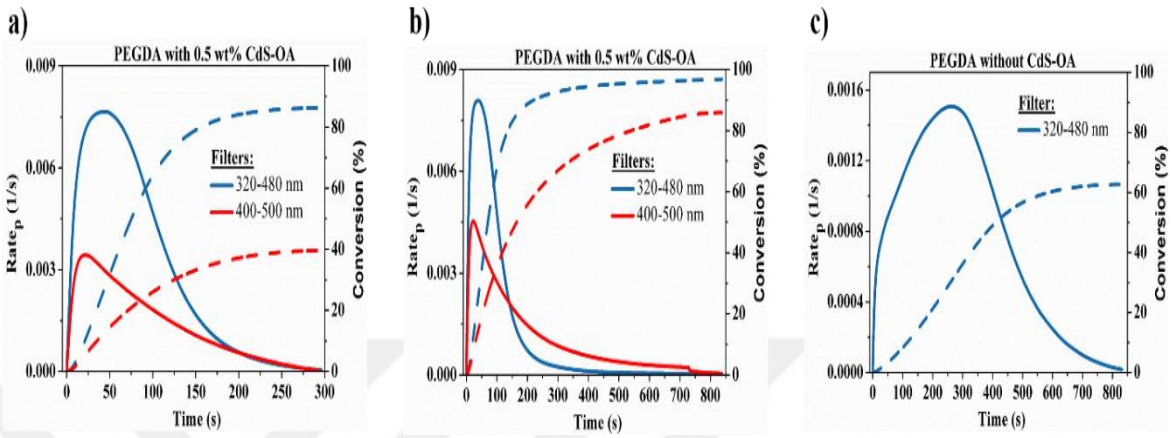

Figure 3.6 Rate of PEGDA polymerization ($Rate_p$: solid lines) and monomer conversion (dashed lines) using 0.5 wt% CdS-OA quantum dots and light intensity of 50 mW cm^{-2} in photo-DSC a) for 5 min b) for 15 min utilizing two different emission filters: 320-480 nm filter (blue color) and 400-500 nm filter (red color). c) Kinetic profile of PEGDA autopolymerization under the same conditions using 320-480 nm filter (blue color).

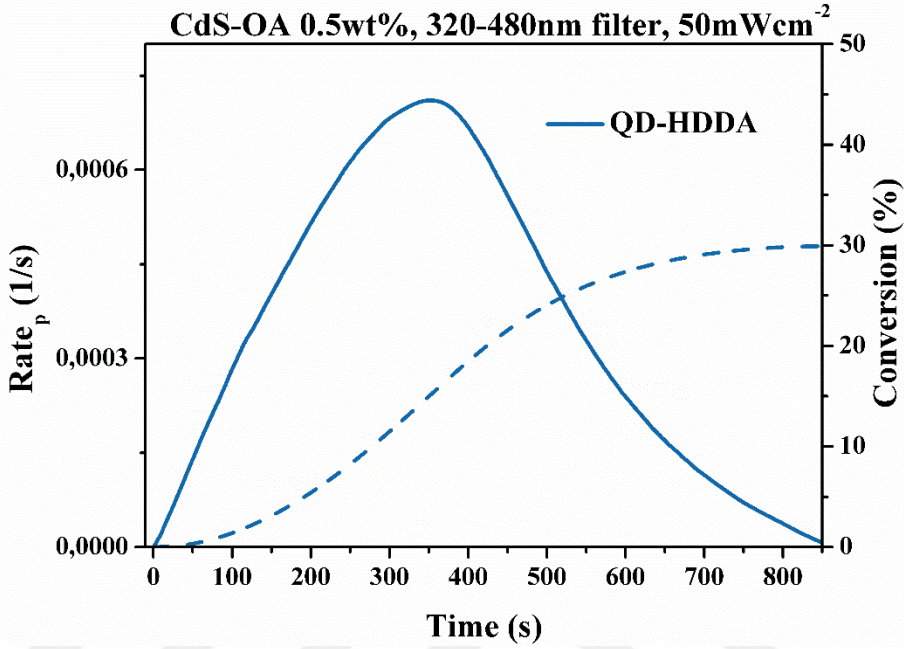

Figure 3.7 Rate of HHDA polymerization ($Rate_p$: solid lines) and monomer conversion (dashed lines) using 0.5 wt% CdS-OA quantum dots and light intensity of 50 mW cm^{-2} in photo-DSC for 15 min utilizing a 320-480 nm emission filter (blue color)

The influence of the reaction volume added to the aluminum pan was studied by photo-DSC using 0.5 wt% CdS-OA and the light intensity of 50 mW cm^{-2} with the 400-500 nm long-wavelength filter for 15 minutes reaction time. In photo-DSC studies, the small volumes are usually studied because the light should be able to penetrate through the sample. **Figure 3.8** illustrates that as the reaction volume increases, the rate of polymerization remained almost the same but the conversion increased slightly. This indicates the standard

procedure (10 μL) we used through phot-DSC studies does not prevent full conversion of the monomer.

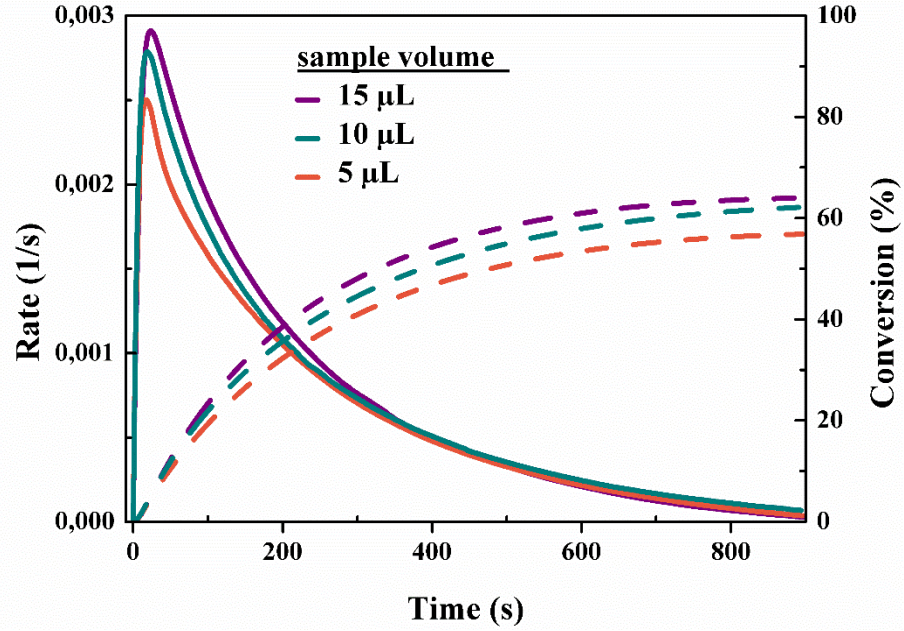

Figure 3.8 The influence of reaction volume to rate and conversion of PEDA studied by photo-DSC using 400-500 nm filter and light intensity of 50 mW cm^{-2}.

3.4 Investigation of the initiating species

Origin of the initiating radical is controversial with QDs. Previous literature indicated ignition from the hole-scavenging molecules such as isopropyl alcohol, TEA or water. Yet, none of these are available in our system. When TEA was added to the typical polymerization mixture a minor difference in the conversion was observed (**Table 3.1**). Hence, the major initiation should be different in this case. In an effort to elucidate the initiation mechanism

and its relation to the coating of the QD, ESR study was performed (**Figure 3.9**). CdS-OA QDs were dissolved in tert-butyl benzene, purged with nitrogen and irradiated at 365 nm for 420 sec. The light generated radicals were then trapped by phenyl-*N*-tert-butylnitrone (PBN) as a spin trap agent and the following hyperfine coupling constants (hfc) were found: a_N = 14.5 G and a_H = 2.5 G. This clearly indicates the formation of a carbon centered radical.

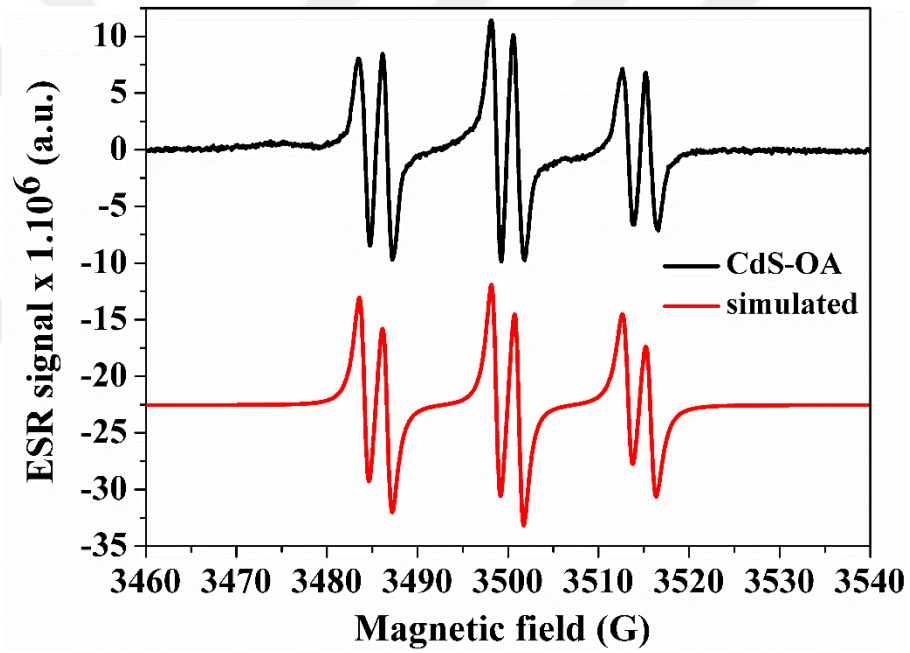

Figure 3.9 ESR spin-trapping experiments with BPN

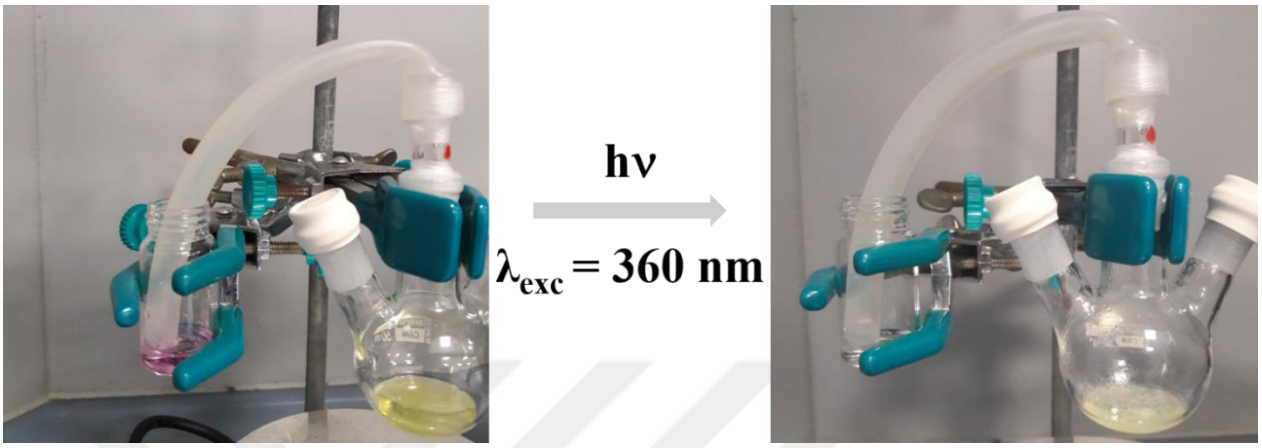

Figure 3.10 Change in the color of sodium carbonate solution with phenolphthalein as a result of decarboxylation upon irradiation at 360 nm

Previously, it was shown that photoinitiation of acrylics can be achieved with fatty acid coated iron oxide nanoparticles and in deed decarboxylation of the fatty acid upon irradiation was responsible from the radical generation. Here, a decarboxylation test was also performed. A flask containing CdS-OA suspended in toluene (15 mg QD in 3.0 mL toluene) was connected to another flask containing aqueous Na_2CO_3 solution (3.1×10^{-4} M) and phenolphthalein via a rubber tubing, then the QD solution was irradiated at 360 nm (100 W lamp, Black ray) (**Figure 3.10**). Not only the pink color of the indicator disappeared but also QDs crashed out of the solution. This does confirm the decarboxylation which would cause first $NaHCO_3$ formation in the receiving tube and subsequent pH drop coupled with discoloration of the indicator. Such decarboxylation of the fatty acid coating of QDs would mean loss of the stabilizing ligand and hence QDs crash out of solution. However, when

irradiation is done in the presence of a monomer, growing polymer obviously stabilize the nanoparticle preventing aggregation and dramatic losses in the optical properties (**Figure 3.2b, c**). These results also agree with the changes observed in the UV and PL (**Figure 3.3**) of the CdS-OA irradiated in the absence of monomer. Loss of the coating molecules from the surface would cause surface defects responsible from non-radiative coupling of the exciton and as a result reduce the emission intensity. Lastly, a control experiment was performed with only OA as a photoinitiator but no polymerization was obtained (**Table 3.1**). This indicates that photo-generated hole of the QD is responsible from the decarboxylation process (**Figure 3.8**).

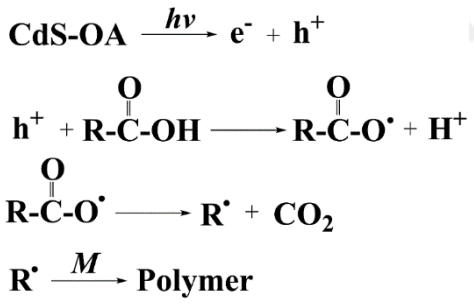

Scheme 3.1 Proposed mechanism of initiation by CdS-OA QDs

In the light of obtained data from ESR and decarboxylation experiments, the mechanism for the initiation was proposed for CdS-OA photoinitiator (**Scheme 3.1**). Upon the irradiation of QDs with UV light, electron and hole separation occurs. The surface stabilizing molecule OA transfers an electron the hole in the VB, resulting in a proton and an unstable radical

which in turn undergo a hemolytic cleavage between a-carbon and carbon atom of carbonyl group. The hemolytic cleavage provides the carbon based initiating radical and also gives off carbon dioxide gas. Finally, the initiating specie starts the polymerization.

3.5 Investigation of Particle Size and Quality on the Performance of CdS-OA QDs as a Photoinitiator

In the former section, it was shown that oleic acid coated CdS QDs are able to successfully initiate the polymerization of MMA, PEGDA and HDDA in toluene. Here, the effect of the first excitonic peak or the size of QDs on efficiency of the initiation will be investigated. Also, how the quality of QDs in terms of the optical properties affects the initiation efficiency will be discussed.

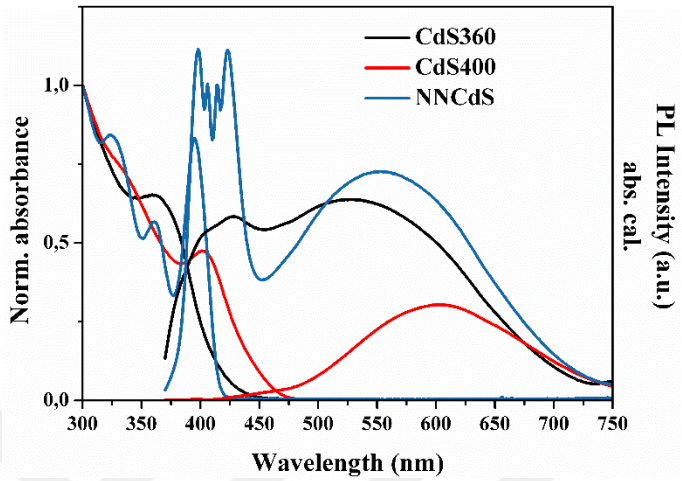

Figure 3.11 Absorbance and absorption calibrated PL spectra of CdS360, CdS400 and NNCdS

Two different oleic acid stabilized CdS QDs were synthesized by changing the OA/Cd ratio. CdS360 coded QDs have the first excitonic peak at ~357 nm and dominant surface-trapped emission at 541 nm (**Figure 3.11**). On the other hand, CdS400 coded QDs show first excitonic peak at 400 nm and dominant surface-trapped emission at 601 nm (**Figure 3.11**). To evaluate QDs' quality, NNCdS coded QDs were purchased from NNCrystal, having first excitonic peak at 400 nm and band gap emission at 409 nm and surface-trapped emission at 551 nm (**Figure 3.11**).

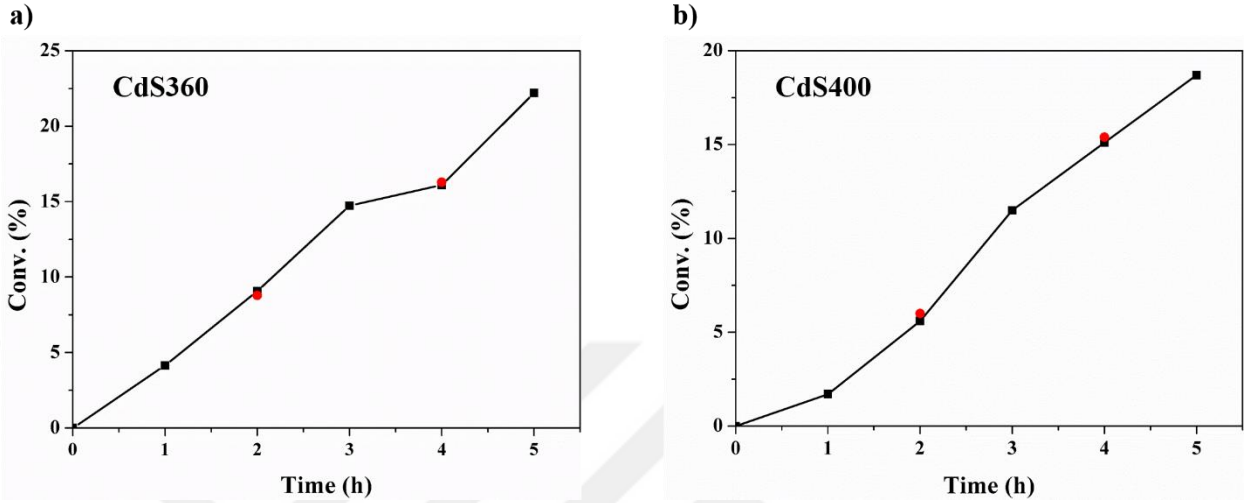

Figure 3.12 Time dependent MMA conversion initiated with different CdS-OAs (Red spheres represent the polymerization solution that is allowed to continue to polymerization in the dark for one more hour). All polymerizations were conducted with 0.5 wt% QD and 2.0 g MMA in Rayonet (λ_{exc} = 365 nm.)

CdS360 and CdS400 QDs were prepared as 5 mg mL^{-1} in toluene and utilized in the photopolymerization of 2.0 gr MMA. As the irradiation time increases from 1 h to 5 h, conversions also increased with both CdS360 and CdS400. However, CdS360 yielded slightly more PMMA than CdS400 at any point within 5 h. For example, in 5 h CdS360 and CdS400 provided 22.2% and 18.7% conversion, respectively (**Figure 3.12**). It means that QD with a first excitonic peak at shorter wavelength works better, at least when excited at 360 nm.[67] In the literature, there are examples of dark polymerization[68], meaning that the polymerization continues after the light was turned off, instead of immediately ceasing

the growth of active chains.[58] To evaluate the presence of dark polymerization, polymerization solutions were kept under dark for 1 h after 2 h and 4 h illuminations. CdS360 provided 9.1% conversion for 2h polymerization and conversion achieved after keeping the replica in the dark for 1 h was 8.8%. This minor difference is probably originating from deviations occurring during the precipitation and purification. The monomer conversion was 16.1% after 4 h irradiation and 16.3% after additional 1 h dark period. In the case of CdS400, 2 h polymerization provided 5.6% conversion and 1 h additional dark period provided 6.0% conversion. In 4 h polymerization of CdS400, the conversion was 15.1 and with additional 1 h in the dark 15.4%. Hence, these data suggest that CdS-OA QDs do not produce any initiating species in the absence of the irradiation and the growing radicals is not long-lived and dies when the light is turned off, providing a well-controlled polymerizations

The QD-PMMA composites were readily soluble in several organic solvents such as toluene and THF. Optical properties of QD-PMMA samples were determined using their dispersion in toluene. Both the first excitonic peak and emission maxima of CdS360-PMMA composite (EPP110) shifted to longer wavelengths: 369 and 558 nm, respectively (**Figure 3.13a**). In the case of CdS400-PMMA composite (EPP114) both positions of the first excitonic peak and the emission maxima are almost identical to those of CdS400 (**Figure 3.13b**). However, in both cases, photopolymerization enhanced the emission intensity of the parent QDs. It might be proposed that the resulting polymer removes the non-emissive

surface traps or makes the non-emissive traps emissive and plus promotes the emissive trap states on the QD surface.

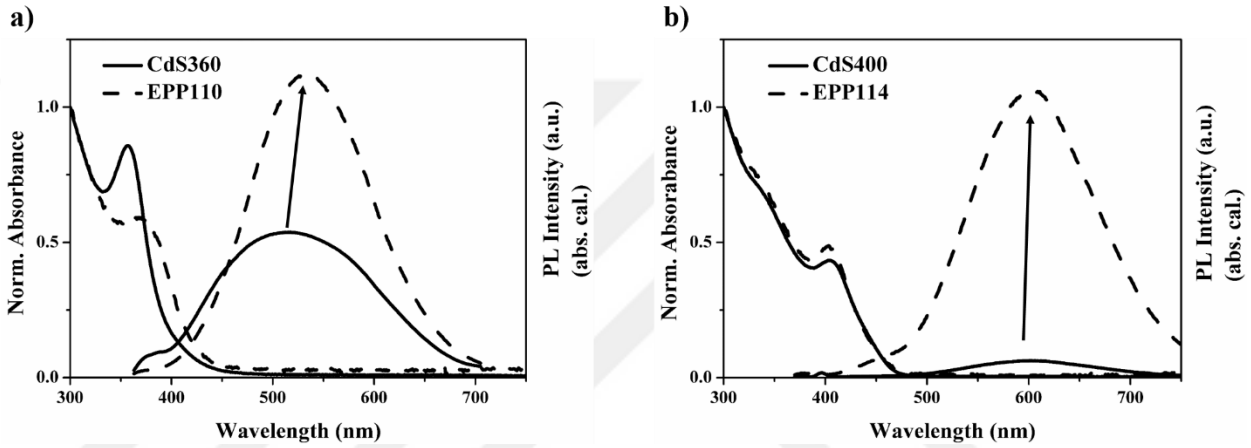

Figure 3.13 Absorbance and Photoluminescence spectra of a) CdS360 and CdS360-PMMA, b) CdS400 and CdS400-PMMA in toluene. QD concentration 5 mg mL^{-1}, λ_{exc} = 365 nm.

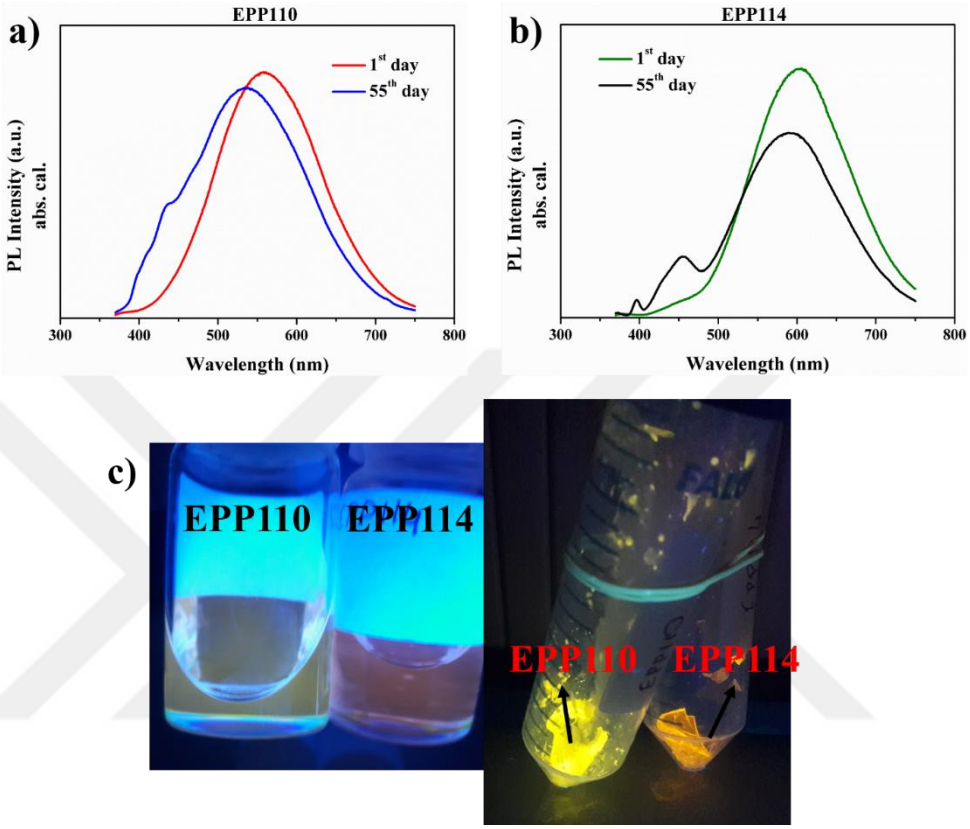

Figure 3.14 Changes in the photoluminescence spectra of a) CdS360-PMMA (EPP110) and b) CdS400-PMMA (EPP114) shortly after synthesis and 55 days later, c) fluorescence of colloidal solutions and composites of EPP110 and EPP114 under UV light

Figure 3.14 shows the change in the PL intensity of QD-PMMA solutions of EPP110 and EPP114 as a function of time. PL intensity of both solution reduced at 55th day after they were dissolved in toluene for the first time and also shifted to shorter wavelengths with an appearance of a shoulder at shorter wavelengths. PL intensity of EPP110 decreased by 6%

while of EPP114 decreased by 26%. These nanocomposites are strongly luminescent as seen in **figure 3.14c**. EPP110 containing CdS360 fluoresce yellow while EPP114 fluoresce orange when excited with a UV lamp (365 nm).

In order to evaluate the reproducibility of the polymerization, three identical polymerization of MMA-QD solutions were prepared using 0.1wt% CdS400 and photo-polymerized simultaneously in Rayonet (**Table 3.3**). MMA conversions obtained from these 3 runs is 19.23% with a standard deviation of 0.109 indicating quite reproducible results.

Table 3.3 Variation among the MMA photopolymerization initiated with 0.1 wt% CdS400

Experiment	**Conversion[a)] [%]**
1	19.17
2	19.17
3	19.36

* Reaction solution: 2.0 mL toluene with 0.1 wt% CdS400 and 2.0 g MMA; λ_{exc} = 365 nm. t_{rxn} = 5 h

a) Conversions were measured gravimetrically. Average = 19.23%, St. dev. = 0.109

Table 3.4 Effect of co-initiator amount on MMA conversion in CdS400 photoinitiated polymerizations*

Experiment	TEA[a)] [wt%]	Conversion[b)] [%]
E0	-	19.36
E1	0.1	19.63
E2	0.5	20.36
E3	1.0	19.61
E4	2.0	20.15

* Reaction solution: 2.0 mL toluene with 0.1 wt% CdS400 and 2.0 g MMA; λ_{exc} = 365 nm. t_{rxn} = 5 h

b) TEA amounts were reported as wt% with respect to 2.0 g MMA.

a) Conversions were measured gravimetrically.

In the literature, quantum dots or wide band-gap semiconductors (i.e. ZnO) have been utilized as photoinitiators in the polymerization of vinyl monomers.[69, 70] In most of the cases, these nanocrystals have been used either in the presence of a hole-scavenging solvent or a co-initiator such as TEA.[57, 58] Upon the excitation of PI, photo-generated electron-hole pairs form and via electron transfer from PI (or sensitizer) to TEA, the initiating radical forms on α–carbon of TEA and starts the polymerization. Here, we also investigated the

effect of the presence of a co-initiator on polymerization of MMA using 0.1 wt% CdS400 as the photoinitiator. Results summarized in **Table 3.4** shows that the presence of TEA in the polymerization solution as a co-initiator has no interference with the photopolymerization. Yet, in order to confirm that this is not related to the quality of the particles or size, comparative polymerizations initiated with CdS360 and NNCdS with only 1.0wt% TEA were also studied.

Table 3.5 MMA conversion and PMMA properties initiated with CdS-OA QDs with or without a co-initiator*

QD	Co-initiator					
	-			TEA		
	Conv.[a] [%]	**M_n [b] [g mol^{-1}]**	**M_w / M_n**	**Conv. [%]**	**M_n [b] [g mol^{-1}]**	**M_w / M_n**
Control 1	-	-	-			
Control 2				3.73	165.5	1.94
CdS360	22.69	94.0	1.71	30.66	61.8	1.51
CdS400	19.36	102.4	1.69	19.61	78.5	1.50
NNCdS	14.43	122.0	1.69	22.90	53.4	1.40

*Reaction solution: 2.0 mL toluene with 0.1 wt% CdS400 and 2.0 g MMA; λ_{exc} = 365 nm; 1.0 wt% TEA as co-initiator, t_{rxn} = 5 h

a) Conversions were measured gravimetrically.

[b)] Number average molecular weight (M_n) and polydispersity index were determined by GPC and M_n values were reported as M_n 10^{-3}.

Table 3.5 shows that no polymer was obtained in 5 h irradiation of MMA solution in toluene in the absence of QD. TEA itself in the absence of QDs provided 3.73% conversion and the resulting polymers had M_n around 165 kDa with the PDI of 1.94. CdS360 resulted in 22.69% conversion while CdS400 provided 19.36% conversion when 0.1 wt% QD was used, similar to results obtained with 0.5 wt% QD concentration (**Figure 3.12)**. Depending on these results, it can be suggested that CdS-OA QDs with the first excitonic peak at shorter wavelength which is right at the excitation wavelength are capable of initiating polymerizations more efficiently than larger QD of the same type. NNCdS and CdS400 QDs have their first excitonic peak at almost same position, but their emission profile are quite different. Thus, these two QDs may reflect the influence of QD quality on photopolymerization. It can be speculated that high quality QDs would perform lower initiation efficiencies since most of the available electrons in CB returns to ground state rapidly by emitting a photon[59], eliminating the possibility of alternative reactions of the photogenerated electrons and holes to form an initiating radical. Indeed, a lower conversion (14.43%) was achieved under identical conditions with NNCdS in comparison to CdS400, supporting such a hypothesis. When TEA was used as a co-initiator with CdS360 or NNCdS, unlike CdS400, an increase from 22.69% to 30.66% with CdS360 and from 14.4% to 22.90%

with NNCdS was obtained. Moreover, the molecular weight analysis of polymers freed from QDs were above the critical molecular weight PMMA

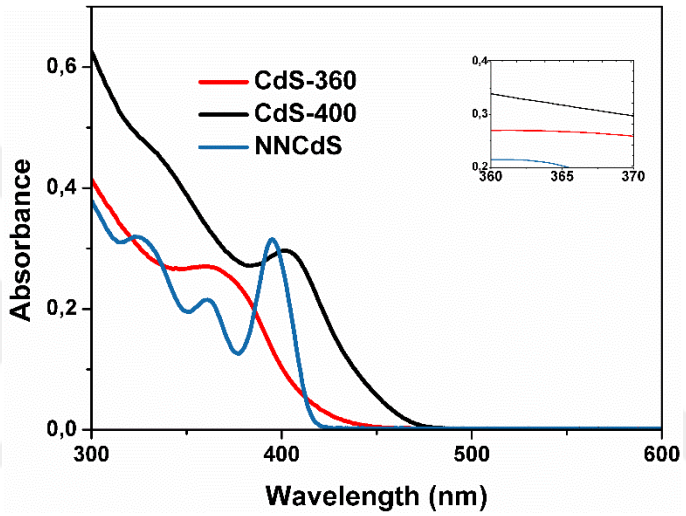

Figure 3.15 Absorbance spectra of CdS360, CdS400 and NNCdS at 62.5 µg mL^{-1}

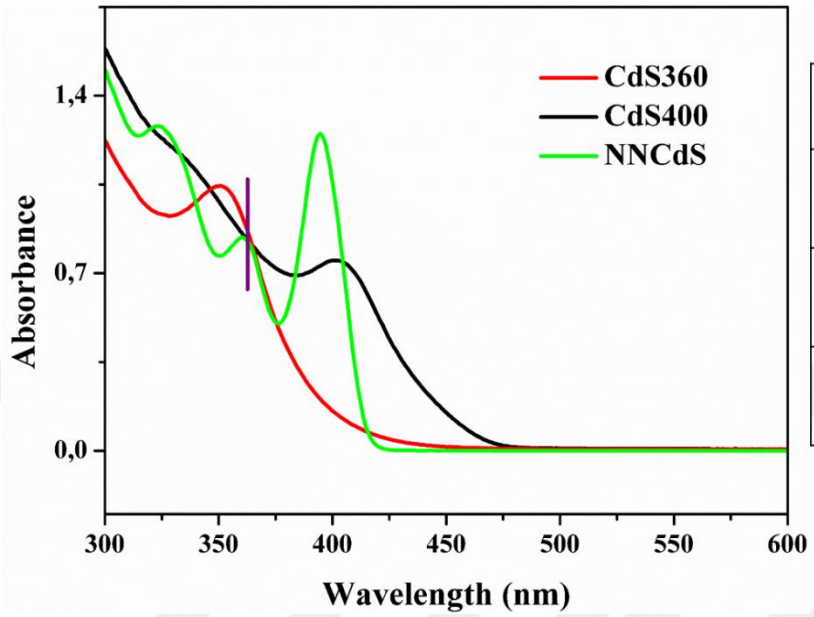

QD	Conv. [%]
CdS360	11.32
CdS400	10.27
NNCdS	7.64

Figure 3.16 Absorbance spectra of QDs with the same amount of absorbance at 365 nm. 2.0 ml of QDs with the same absorbance at 365 nm and 2.0 g MMA were polymerized for 5 h using Rayonet (λ_{exc} = 365 nm). Conversions were calculated gravimetrically.

In batch polymerization, Rayonet with 18 UV lamps (365 nm), was utilized as a light source. **Figure 3.15** shows the absorbance spectra of QDs at the same concentration of 62.5 μg mL^{-1} since in comparative experiments QD concentration was kept constant. When the absorbance at 365 nm were compared at identical conditions, CdS400 had the highest absorbance and NNCdS400 has the lowest while CdS360 in the middle. Thus, the number of photons absorbed upon excitation at 365 nm practically will be higher in CdS400 producing more excitons compared to others, in a way, which can result in the formation of free radicals.

Hence, one may suggest that CdS400 provides higher conversions due to higher absorbance at the excitation wavelength. To understand the role of absorbance at the excitation wavelength, photopolymerization of MMA was performed with these three QDs at a concentration where their absorbance at 365 nm are identical (**Figure 3.16**). CdS400 provided a higher conversion (10.27%) than NNCdS (7.64%). *This result points out that QDs with the same core, same composition, almost same first excitonic peak and absorbance at the excitation wavelength but with different quality exhibit different efficiency as PIs, and QDs with more defect states work better*. Comparing QDs with the same core and coating but different size would not make a sense since QD with larger size had a higher absorbance and lower conversion at the same concentration. To sum up, QDs with lower size and lower quality perform better efficiencies as PIs.

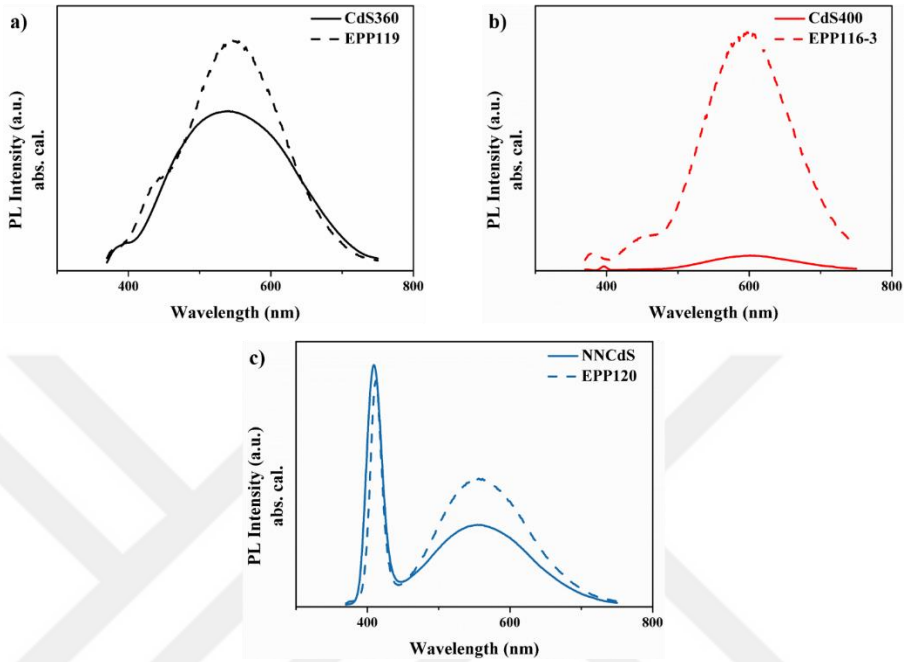

Figure 3.17 Absorption calibrated PL intensities of a) CdS360 and CdS360-PMMA (EPP119), b) CdS400 and CdS400-PMMA (EPP116-3), c) NNCdS and NNCdS-PMMA (EPP120). All QD-PMMA composites were obtained using 0.1 wt% QD as photoinitiator given in table 3.5.

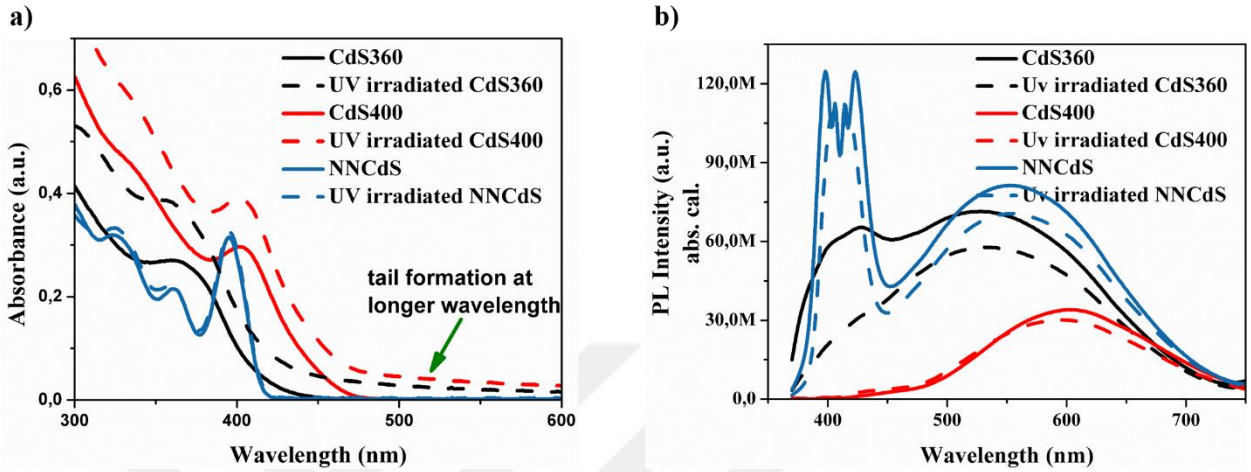

Figure 3.18 a) Absorbance spectra of fresh and UV irradiated QDs and b) absorption calibrated PL spectra of fresh and 5h UV irradiated QDs

Similar to the results reported for QD-PMMA produced with 5 mg mL^{-1} QD concentration (Figure 3.13), when polymerizations were initiated with 0.1 wt% QD, an increase in the luminescence intensity for all QD-PMMA samples compared to the initiating QD (**Figure 3.17**) It seems like trap state emission is increased after photopolymerizations. The most dramatic enhancement was observed in cased of CdS400. The strong band-gap emission of NNCdS is comparable to the native NNCdS but, the surface-trap emission increased significantly after the polymerization (**Figure 3.17c**) In a most basic sense, there could be two reasons for this: 1. Formation of PMMA around QDs and 22. Photopolymerization event itself. Therefore, QD-toluene solutions at 62.5 µg mL^{-1} were irradiated 5h in the Rayonet and the absorbance and photoluminescence spectra before and after irradiation were compared (**Figure 3.18)**. NNCdS seems to be very resistant to irradiation since no change in the

absorbance spectra with a slight decrease in the trap-state emission component were detected. In case of CdS360 and CdS400, although no remarkable shift in the first excitonic peak position was observed, there is a tail at the longer wavelengths. This may be due to the loss of fatty acid coating and aggregation to a certain extent as discussed previously. In all samples, a slight decline in the trap emissions was observed, not an increase. Thus, the observed enhancement of the luminescence intensity of QDs after photopolymerization is mostly related to PMMA formation around QDs, but not the UV irradiation itself.

3.6 Investigation of the QD size and Quality on Photopolymerization kinetics

The kinetics of the photopolymerizations initiated with CS360, CdS400 and NNCdS were studied by photo-DSC using PEGDA as a monomer with two different filter sets: 320-480 nm covering a large window from UV to visible region and 400-500 nm long wavelength filter. All reactions were performed with 0.1 wt% QD. A typical reaction mixture was prepared by mixing 200 μL of 1.0 mg mL^{-1} QD solution in toluene and 0.2 gram PEGDA. 10 μL of this mixture was added to the sample pan. Each reaction was repeated 3 times to observe the standard deviation between the experiments.

Excitation of the polymerization mixture between 320-480 nm at a light intensity of 30 mW cm^{-2} (Figure 3.21) showed quite high monomer conversions in 5 min (**Figure 3.21**). Average double bond conversion was calculated as 85.2% with CdS360, 82.0% with CdS400 and 97.8% with NNCdS.

The shortest average time to exotherm maxima was 43.3 s with CdS360 where 35.5% conversion was also achieved. This was 53.0 s with 41.1% conversion in case of NNCdS and 73.5 s with a 37.5% with CdS400. Besides, rate of polymerization in case of CdS360 and NNCdS are quite similar: 0.010 and 0.011 s^{-1}, respectively. However, the rate obtained by CdS400 at the peak maximum was almost 50% slower that of CdS360 and NNCdS with a value of 0.006 s^{-1}.

When the intensity of the light was increased to 50 mW cm^{-2} faster polymerizations and higher conversions were achieved (**Figure 3.20)** under otherwise identical conditions. Time to peak maxima was as fast as 34.4 s with 38.3% double bond conversion with CdS360 (**Figure 3.20a** 37.6 s with a 40% conversion with NNCdS (**Figure 3.20c**) and 55.8 s with 36.9% with CdS400 (**Figure 3.20b**). Parallel to this, photopolymerization rates obtained at the peak maximum are higher at higher excitation power, as well: 0.015, 0.014 and 0.008 1/s for NNCdS, CdS360 and CdS400, respectively. Overall conversions also increased to 99.6, 94.3 and, 87.5% with NNCdS, CdS360 and CdS400, respectively. To sum, increasing the light intensity shortens the time needed to achieve the peak maximum and increases the polymerization rate, and hence the double bond conversion.

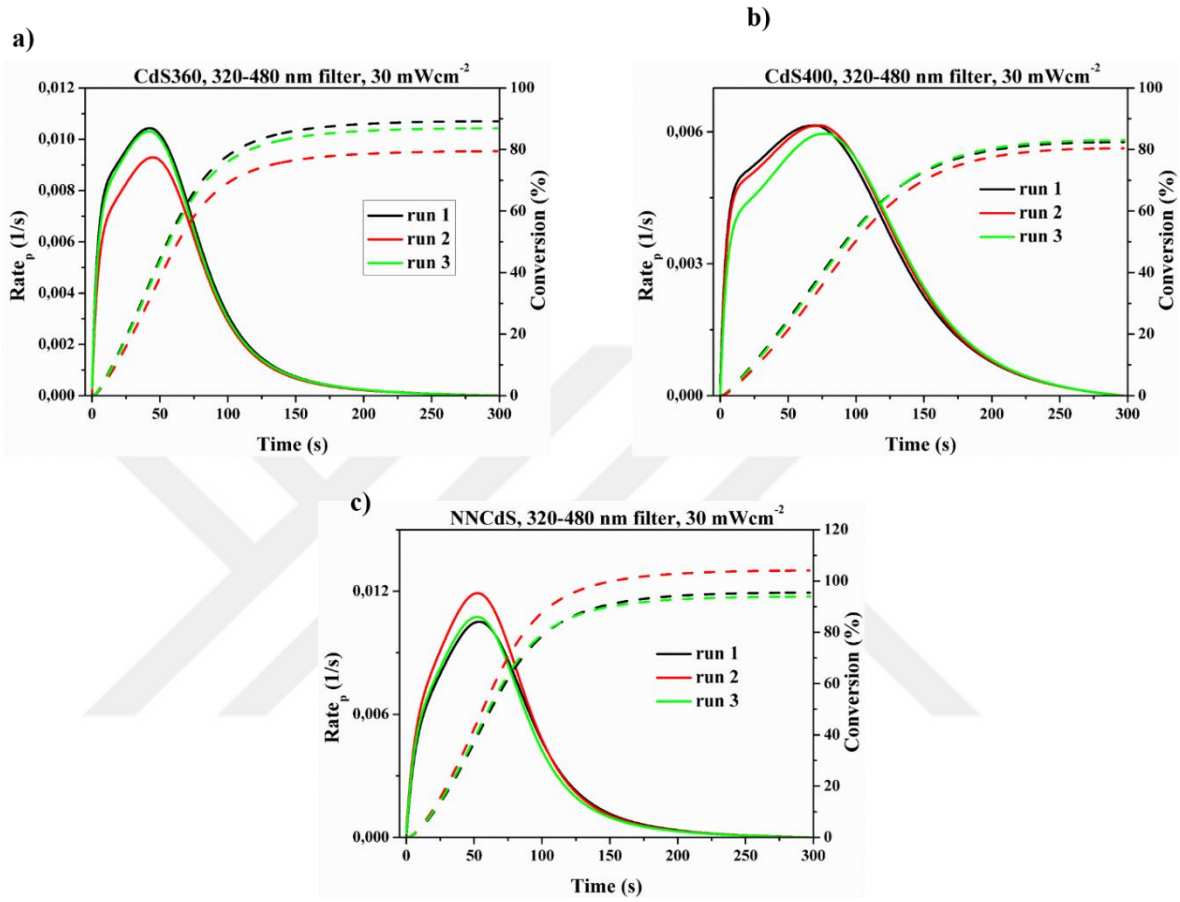

Figure 3.19 Rate of PEGDA photopolymerization ($Rate_p$: solid lines) and monomer conversion (dashed lines) using 0.5 wt% QDs at a light intensity of 30 mW cm^{-2} in photo-DSC. QDs used as PI are of a) CdS360, b) CdS400 and c) NNCdS initiated PEGDA. Each were run three times

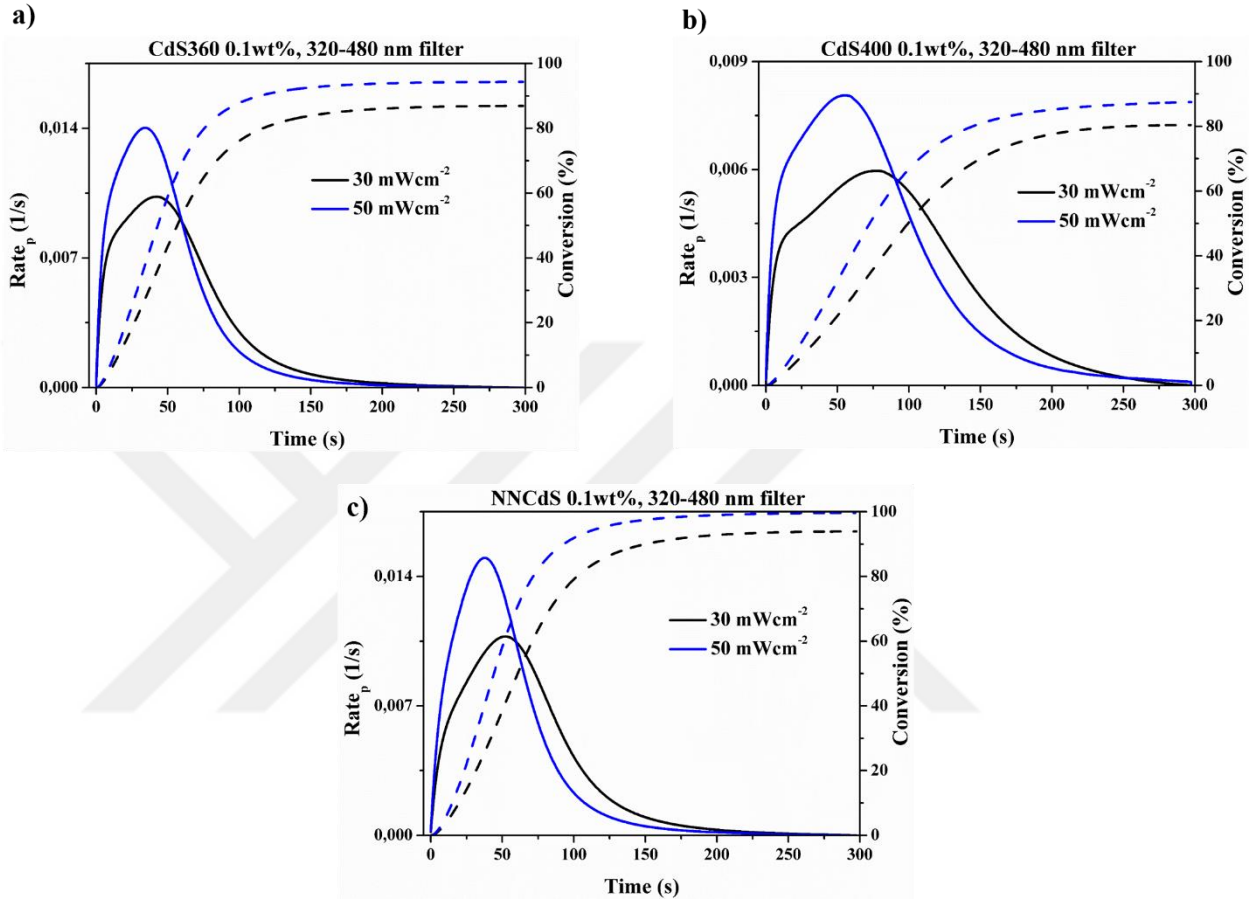

Figure 3.20 Influence of the light intensity on the rate ($Rate_p$: solid lines) and conversion (dashed lines) of photopolymerization of PEGDA using 0.1 wt% QDs with 320-480 nm filter. Blue color represents the light intensity of 50 mW cm^{-2}, while black color representing the light intensity of 30 mW cm^{-2}.

When these three QDs were compared, kinetic studies indicate that NNCdS and CdS360 behave similar but the slowest rate and lowest conversion with CdS400 which is an opposite to the results obtained from the batch reactions.

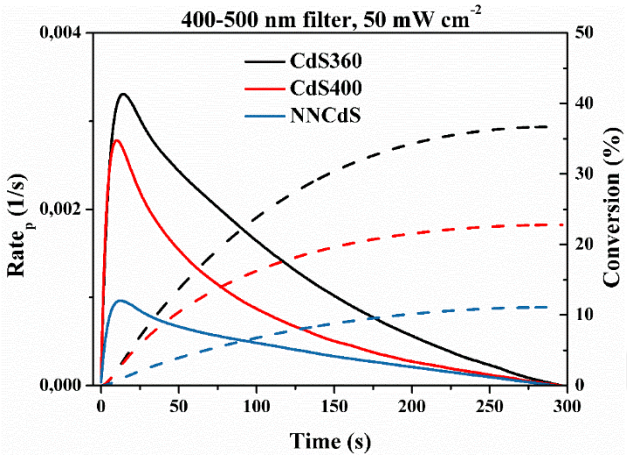

Figure 3.21 Rate ($Rate_p$: solid lines) of photopolymerization and double bond conversion (dashed lines) of PEGDA using 0.1 wt% QDs with 400-500 nm filter and the light intensity of 50 mW cm^{-2}.

One of the major motivations in using QDs as PI is absorbance at long wavelength and hence their potential as long-wavelength PI. Therefore, these three QDs (0.1 wt%) were also used for photoinitiated polymerization of PEGDA using 400-500 nm excitation filter with a light intensity of 50 mW cm^{-2}. All QDs, although the first excitonic peaks were located at ~360 nm for CdS360 and ~400 nm for CdS400 and NNCdS, have a tail on their absorbance

spectra projecting into the 400-500 nm interval. In addition to the tail, all QDs exhibits surface-trap emissions at the longer wavelengths. This might be thought as there are trap energy levels within the bandgap and electrons might be excited to those states with excitation at longer wavelengths.

All QDs provided photoinitiation at 400-500 nm excitation as seen in **Figure 3.22.** Rate of photopolymerization and the double bond conversion was highest with CdS360 and lowest with NNCdS. Monomer conversions were 36.7, 22.8 and 11 % with CdS360, CdS400 and NNCdS, respectively. Interestingly, CdS360 has the highest and NNCdS has the lowest absorption within 400-500nm range, indicating that it is not only the amount of adsorbed photons which influences the photopolymerization rate. Although these conversions are much lower than those obtained with 320-480 nm filter, results are still promising for the development of long wavelength photoinitiators. For example, higher QD concentration and light intensity would increase the rate and the conversion.

Table 3.6 Summarization of photo-DSC studies using CdS360, CdS400 and NNCdS

QD Type	Light Intensity (mW cm^{-2})	Excitation filter (nm)	Time to peak (s)	Double bond Conversion at peak maxima [%]	Double bond Conversion after 5 min [%]	Rate at peak maxima
CdS360	30	320-480	43.3	35.5	85.2	0.010
CdS400	30	320-480	73.5	37.5	82.0	0.006
NNCdS	30	320-480	53.0	41.1	97.8	0.011
CdS360	50	320-480	34.4	38.3	94.3	0.014
CdS400	50	320-480	55.8	36.9	87.5	0.008
NNCdS	50	320-480	37.6	40	99.6	0.015
CdS360	50	400-500	14.2	3.5	36.7	0.00331
CdS400	50	400-500	10.0	2.1	22.8	0.00278
NNCdS	50	400-500	12.0	0.86	11.0	0.00096

4. Comparison of Core and Core-Shell Quantum Dots as PI in Free Radical Polymerization of vinyl monomers

It is known that core/shell structures usually are more stable compared to just core semiconductors and have higher quantum yield. Theoretically, shell passivates the surface and removes surface defects which may cause non-radiative relaxation of the photoexcited electron. Also, it traps the photogenerated exciton within the core, hence lowers its interaction with the surrounding. Therefore, studying photoinitiation with a simple core type and a core/shell type QD may contribute significantly to our understanding of the initiation mechanism.

It is difficult to find core and core/shell nanoparticle with the same excitonic peak position with CdS due to the quantum confinement effect (**Scheme 4.1**).[12] But, there are such compositions of CdSe coated with octadecylamine (ODA). Hence, two CdSe-ODA and CdSe-ZnS-ODA with different crystal sizes and the first excitonic peaks at 540 nm and 620 nm were purchased from the NNCrystal (**Figure 4.1**).

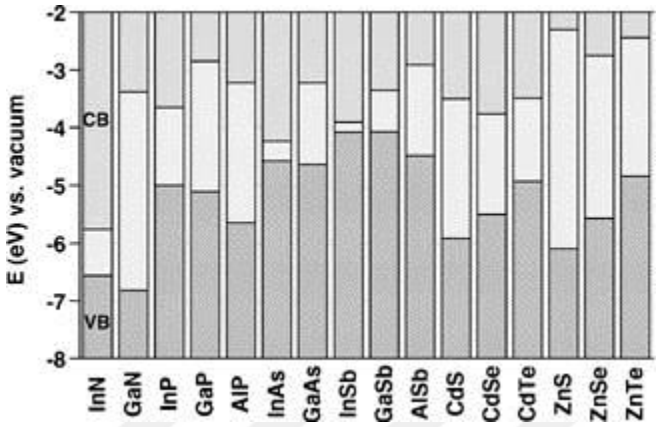

Scheme 4.1VB and CB potentials of widely used semiconductors [12]

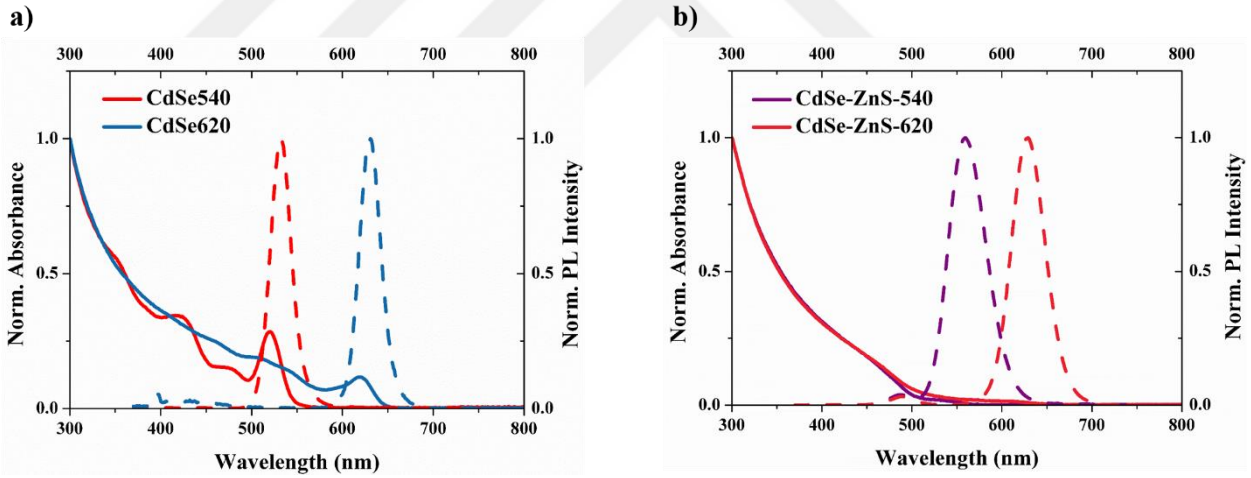

Figure 4.1 Normalized UV and PL spectra of a) CdSe-ODA QDs and b) CdSe-ZnS-ODA core-shell QDs

Typical batch polymerization procedure used in the previous section for the MMA photopolymerization initiated by CdS-OA QDs was also followed for the CdSe and CdSe-ZnS initiated photopolymerizations of MMA (**Table 4.1**). Indeed, we were expecting to show

no polymerization with CdSe-ZnS QDs due to the confinement of photogenerated electrons and holes within the core. However, obtaining no polymers in the reactions initiated with CdSe QDs was unexpected. In the previous section, we showed the successful MMA polymerizations induced by oleic acid stabilized CdS QDs of different sizes and quality. These CdSe based QDs have strong absorbance at 360 nm just like CdS-OA but both the core and the coating is different. The reasons of failure in the initiation could be the use of different core (CdSe) with first excitonic peaks at longer wavelengths (540 nm and 620 nm) in comparison to CdS QDs (~360 nm and 400 nm) or the use of different coating material (ODA). Unfortunately there is no commercially available CdSe with OA coating and no CdSe-ODA with first excitonic peak at around 360 nm to study the effect of these two separately. Indeed, influence of the coating on PI efficiency of QDs is also one of the important questions.

Israeli *et al.* investigated the photo-physical role of CdSe-ZnS core-shell QDs in photopolymerization of acrylates initiated with eosin and a tertiary amine co-initiator .[71] They observed slower photopolymerizations when QDs were added to the mixture. Although not clear about the reason, absorbance of the incident light not only by the initiator and co-initiator but also by QDs, adsorption of tertiary amine co-initiator on QD surface and losing its activity are some hypothesis that they have proposed. Photoinitiation with CdSe-ODA and CdSe-ZnS-ODA in the presence of TEA was also studied (Table 4.1). This produced a very small amount of polymer with all four CdSe based QDs but conversions were below

2%, indicating may be formation of some radical species but no efficient photopolymerization. TEA alone can provide 4% monomer conversion under identical conditions (365 nm excitation for 5 h). So, CdSe based QDs may be quenching free radicals formed even by other species such as TEA.

Table 4.1 *Photopolymerization of MMA using CdSe-ODA and CdSe-ZnS-ODA QDs with and without a co-initiator**

QD	Co-initiator	
	-	TEA[a)]
	Conv.[b)] [%]	Conv.[b)] [%]
CdSe-540	-	1.37
CdSe-620	-	1.31
CdSe-ZnS-540	-	1.17
CdSe-ZnS-620	-	0.13

* Reaction solution contains 0.1 wt% QD and 2.0 g MMA. Reaction solution was irradiated in Rayonet for 5 h.

[a)] 1.0 wt% TEA as co-initiator was used with respect to 2.0 g MMA.

[b)] Conversions were calculated gravimetrically.

Kinetic studies performed with PEGDA in photoDSC using 320-480 nm filter and the light intensity of 50 mW cm^{-2} supported this observation (**Figure 4.2**) Indeed, CdSe based QDs could not compete with the autopolymerization of PEGDA at long irradiation times.

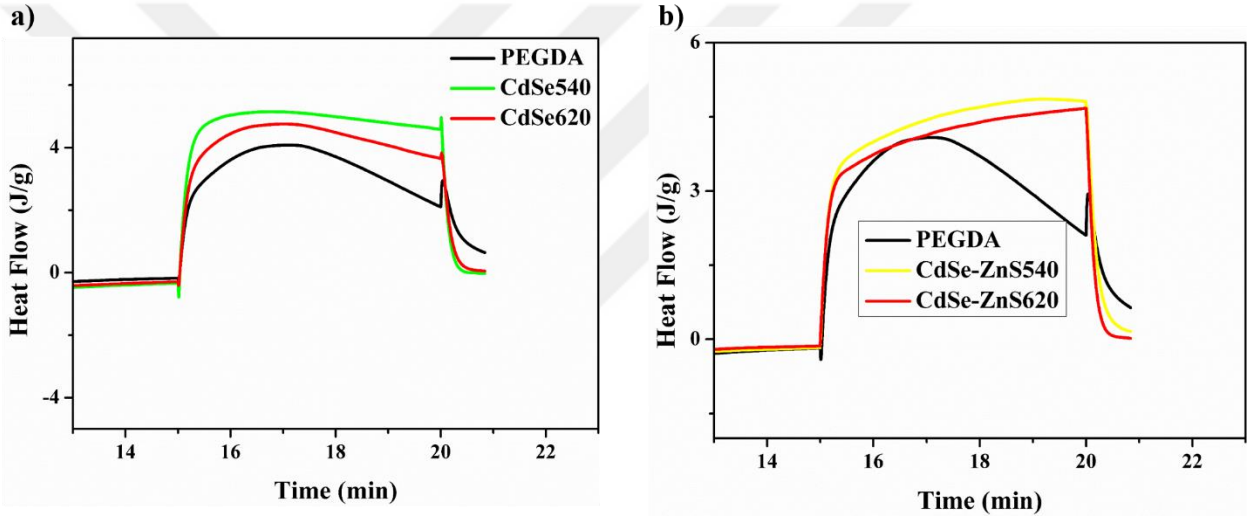

Figure 4.2 DSC thermograms showing a) auto-polymerization of PEGDA (black line), CdSe540 initiated polymerization of PEGDA (green line) and CdSe620 initiated polymerization of PEGDA (red line). b) CdSe-ZnS540 initiated polymerization of PEGDA (yellow), CdSe-ZnS620 initiated polymerization of PEGDA (red).

5. Conclusions

In the first part of the study, explained in Chapter 3.1, the photo-induced polymerization of MAA in toluene using colloidal CdS-OA quantum dots as photo-initiator and irradiation at 365 nm provided colloidal CdS-PMMA hybrid structures in the absence of a co-initiator such as TEA or a hole-scavenging solvent such as water or an alcohol. These CdS-PMMA nanostructures can be dispersed in organic solvents such as toluene to form quite stable colloidal nanostructures with very small hydrodynamic size. They retained the luminescence property of the native quantum dot with enhanced QD photostability. Monomer conversion increases with the reaction time and QD concentration and 0.5 wt% QD is determined as the optimum concentration of PI. PMMA reached high molecular weight (44-66 kDa) with typical T_g in the range of 102-119 °C indicating successful polymerization. Lower T_g of QD-PMMA indicates homogenous distribution of QDs in the polymer and enhanced free volume.

Photo-DSC studies of QD initiated PEGDA photopolymerization using 320-480 nm and 400-500 nm filters indicated higher monomer conversion with the first filter but more than 80% conversion with no autopolymerization of the PEGDA in 15 min with 50 mW cm^{-2} with the second one. This proves CdS-OA as a promising long-wavelength initiator.

ESR studies coupled with decarboxylation test suggest photo-induced decarboxylation of OA coating generating an alkyl radical as the possible source of the initiating radical. This initiation mechanism allows polymerization of hydrophobic monomers more readily since alcoholic solvents or hydrophilic solvents is not required. Hence, many different QD/polymer compositions can be attempted in the future. The long-wavelength initiation, small colloidal hybrid structure, maintenance of the QD luminescence is very practical from the application perspective.

In the later parts of the Chapter 3, the role and the influence of QD size and quality on the photoinitiator efficiency was studied with two home-made CdS-OA QDs of different sizes and a commercial CdS-OA. In general, in case of home-made CdS-OA, the smaller size worked better. But more importantly, these studies suggested that the particle quality or in a way the presence of defect states are more important. The commercial CdS-OA which is denoted as NNCdS with the first excitonic peak at 400 nm gave the lowest MMA conversion in the batch reactions but provided the fastest reactions with highest conversions in the photoDSC studies performed with PEGDA. Origin of this discrepancy between the trend seen in the batch versus photoDSC studies is not clear yet. Photoluminescence decay time, CB and VB position of these QDs as well as monomers need to be determined for a conclusive remark. In future, photoDSC studies need to be performed may be with a methacrylate derivative to eliminate the intrinsic difference between methacrylates versus acrylates. All of these CdS-PMMA nanocomposites are also colloidally stable and have

dramatically stronger luminescence intensity at about the same wavelengths with the parent QD. According to the control experiments, this enhancement in the luminescence intensity is related to the interaction of PMMA with CdS.

In Chapter 4, we aimed to investigate the role and influence of core-shell QDs on photoinitiation in order to clarify the mechanism further. For this purpose in order to have comparable samples and minimize batch to batch variation, commercial core and core-shell QDs with excitonic peaks at the same wavelength were purchased. Since CdS and CdS-ZnS pairs are unavailable commercially, CdSe and CdSe-ZnS QDs stabilized with ODA were purchased in two different sizes with first excitonic peak at 540 and 620 nm. Yet, none of these particles were able to initiate MMA polymerization in batch reactions at 360nm irradiation. Addition of a TEA did not make a dramatic change. PhotoDSC studies performed with PEGDA supported this finding. On the other hand, it seems like some radical formation is taking place with TEA in the batch polymerization of MMA but quenches quickly providing monomer conversion less than 2% which is worse than what TEA can do alone. Also, in photo-DSC studies, these QDs reduced the autopolymerization of PEGDA as well. These suggest that CdSe based QDs with ODA coating may be somehow quenching radicals. This needs to be studied further. ESR studies may help to understand if radicals are forming and what is the nature of these radicals when CdSe based QDs are used.

Overall, in this thesis study, the initiation mechanism of photopolymerization using CdS-OA QDs was found out and first QD based photoinitiation in the absence of a co-initiator, water or alcohol was achieved. It was shown that for successful polymerization, luminescence does not need to be quenched and colloidal polymer/QD nanostructures can be very easily prepared by this method. Polymer properties and luminescence properties indicate interaction between the two components which reduces the Tg somewhat but enhances the luminescence of the QDs was understood and ensured by experimental evidence. CdS-OA QDs have been showed as a promising photoinitiators for long-wavelength initiation. Yet, it seems like pushing the absorbance onset to longer wavelengths may not necessarily mean that initiation wavelength can be pushed to longer values, as well. Defect states seems to a critical factor in the initiation. Besides, the core composition and the coating is shown as important factors that needs to be decoupled in future.

Based on these conclusions, a follow up study should involve:

1. An ESR study with all of these QDs to elucidate if radicals are formed with each has the same nature or if radicals are formed at all, especially in case of CdSe based QDs.
2. Synthesis of home-made CdSe-OA and CdS-ODA to elucidate the impact of core composition and the nature of the coating. Alternatively, ODA may be exchanged with OA before photopolymerizations.

3. Cyclic voltammetry experiments need to be performed in order to determine the CB and VB positions of these QDs as well as the ox-red potential of the monomers and the coating materials.
4. TEGDMA (tetraethyleneglycol dimethacrylate) can be used in photoDSC to have a relatively comparable double bond energy and polymerization kinetic to MMA.
5. A variety of monomers can be utilized to develop variety of nanocomposites such as PEGMA, HEMA, and DMAEMA for biomedical use.

Bibliography

1. Alivisatos, A.P., *Semiconductor clusters, nanocrystals, and quantum dots.* Science, 1996. **271**(5251): p. 933-937.
2. Kamat, P.V., *Quantum Dot Solar Cells. Semiconductor Nanocrystals as Light Harvesters.* Journal of Physical Chemistry C, 2008. **112**(48): p. 18737-18753.
3. Nozik, A.J., *Quantum dot solar cells.* Physica E-Low-Dimensional Systems & Nanostructures, 2002. **14**(1-2): p. 115-120.
4. Michalet, X., et al., *Quantum dots for live cells, in vivo imaging, and diagnostics.* Science, 2005. **307**(5709): p. 538-544.
5. Zrazhevskiy, P., M. Sena, and X. Gao, *Designing multifunctional quantum dots for bioimaging, detection, and drug delivery.* Chemical Society Reviews, 2010. **39**(11): p. 4326-4354.
6. Zhang, F., et al., *Brightly luminescent and color-tunable colloidal CH3NH3PbX3 (X= Br, I, Cl) quantum dots: potential alternatives for display technology.* ACS nano, 2015. **9**(4): p. 4533-4542.
7. Guo, Y.M., et al., *Facile synthesis of stable cadmium sulfide quantum dots with good photocatalytic activities under stabilization of hydrophobic amino acids.* Materials Letters, 2012. **74**: p. 26-29.

8. Samadi-maybodi, A., F. Abbasi, and R. Akhoondi, *Aqueous synthesis and characterization of CdS quantum dots capped with some amino acids and investigations of their photocatalytic activities.* Colloids and Surfaces a-Physicochemical and Engineering Aspects, 2014. **447**: p. 111-119.

9. Shi, L., et al., *Synthesis and application of quantum dots FRET-based protease sensors.* Journal of the American Chemical Society, 2006. **128**(32): p. 10378-10379.

10. Chan, W.C.W., et al., *Luminescent quantum dots for multiplexed biological detection and imaging.* Current Opinion in Biotechnology, 2002. **13**(1): p. 40-46.

11. Rogers, B., J. Adams, and S. Pennathur, *Nanotechnology: understanding small systems*. 2014: Crc Press.

12. Reiss, P., M. Protiere, and L. Li, *Core/Shell Semiconductor Nanocrystals.* Small, 2009. **5**(2): p. 154-168.

13. Brus, L.E., *Electron Electron and Electron-Hole Interactions in Small Semiconductor Crystallites - the Size Dependence of the Lowest Excited Electronic State.* Journal of Chemical Physics, 1984. **80**(9): p. 4403-4409.

14. Rossetti, R., et al., *Size Effects in the Excited Electronic States of Small Colloidal Cds Crystallites.* Journal of Chemical Physics, 1984. **80**(9): p. 4464-4469.

15. Ioannou, D. and D.K. Griffin, *Nanotechnology and molecular cytogenetics: the future has not yet arrived.* 2010, 2010.

16. Klimov, V.I., et al., *Electron and hole relaxation pathways in semiconductor quantum dots.* Physical Review B, 1999. **60**(19): p. 13740-13749.

17. Wardle, B., *Principles and applications of photochemistry*. 2009: John Wiley & Sons.

18. Efros, A.L., et al., *Band-edge exciton in quantum dots of semiconductors with a degenerate valence band: Dark and bright exciton states.* Physical Review B, 1996. **54**(7): p. 4843-4856.

19. Mansur, H.S., *Quantum dots and nanocomposites.* Wiley Interdisciplinary Reviews-Nanomedicine and Nanobiotechnology, 2010. **2**(2): p. 113-129.

20. van Dijken, A., et al., *The Kinetics of the Radiative and Nonradiative Processes in Nanocrystalline ZnO Particles upon Photoexcitation.* The Journal of Physical Chemistry B, 2000. **104**(8): p. 1715-1723.

21. Wu, F., et al., *Radiative and nonradiative lifetimes of band edge states and deep trap states of CdS nanoparticles determined by time-correlated single photon counting.* Chemical Physics Letters, 2000. **330**(3): p. 237-242.

22. http://www.sigmaaldrich.com/catalog/product/aldrich/662410. *core type quantum dots*.

23. Majetich, S. and A. Carter, *Surface effects on the optical properties of cadmium selenide quantum dots.* The Journal of Physical Chemistry, 1993. **97**(34): p. 8727-8731.

24. Ghosh Chaudhuri, R. and S. Paria, *Core/shell nanoparticles: classes, properties, synthesis mechanisms, characterization, and applications.* Chemical reviews, 2011. **112**(4): p. 2373-2433.

25. Huang, C.-P., Y.-K. Li, and T.-M. Chen, *A highly sensitive system for urea detection by using CdSe/ZnS core-shell quantum dots.* Biosensors and Bioelectronics, 2007. **22**(8): p. 1835-1838.

26. Dabbousi, B.O., et al., *(CdSe) ZnS core− shell quantum dots: synthesis and characterization of a size series of highly luminescent nanocrystallites.* The Journal of Physical Chemistry B, 1997. **101**(46): p. 9463-9475.

27. Carothers, W.H., *Polymerization.* Chemical Reviews, 1931. **8**(3): p. 353-426.

28. Flory, P.J., *Principles of polymer chemistry*. 1953: Cornell University Press.

29. Odian, G., *Principles of polymerization*. 2004: John Wiley & Sons.

30. http://polymerdatabase.com/polymer%20chemistry/Chain%20versus%20Step%20Growth.html. *chain-growth versus step-growth polymerization*.

31. Young, R.J. and P.A. Lovell, *Introduction to polymers*. 2011: CRC press.

32. Flory, P.J., *Intramolecular reaction between neighboring substituents of vinyl polymers.* Journal of the American Chemical Society, 1939. **61**(6): p. 1518-1521.

33. Vasishtha, R. and A. Srivastava, *Mechanistic and kinetic studies of the polymerization of styrene photoinitiated by p-acetyl benzylidene triphenylarsonium*

ylide. Journal of Photochemistry and Photobiology A: Chemistry, 1989. **47**(3): p. 379-383.

34. Kaur, M. and A. Srivastava, *Synthesis of arsenic containing polymethylmethacrylate using p-acetyl benzylidene triphenyl arsonium ylide as photoinitiator*. Journal of Photochemistry and Photobiology A: Chemistry, 1998. **119**(1): p. 67-72.
35. Yagci, Y., S. Jockusch, and N.J. Turro, *Photoinitiated polymerization: advances, challenges, and opportunities.* Macromolecules, 2010. **43**(15): p. 6245-6260.
36. Oster, G. and N.-L. Yang, *Photopolymerization of vinyl monomers.* Chemical Reviews, 1968. **68**(2): p. 125-151.
37. Johnston, D.S. and D.C. Pepper, *Polymerisation via macrozwitterions, 3. Ethyl and butyl cyanoacrylates polymerised by benzyldimethyl, triethyl and tribenzylamines.* Macromolecular Chemistry and Physics, 1981. **182**(2): p. 421-435.
38. Palmer, B.J., et al., *A new photoinitiator for anionic polymerization.* Macromolecules, 1995. **28**(4): p. 1328-1329.
39. Kutal, C., P.A. Grutsch, and D.B. Yang, *A novel strategy for photoinitiated anionic polymerization.* Macromolecules, 1991. **24**(26): p. 6872-6873.
40. Stansbury, J.W., *Curing dental resins and composites by photopolymerization.* Journal of esthetic and restorative dentistry, 2000. **12**(6): p. 300-308.
41. Nunes, T.G., et al., *Spatially resolved photopolymerization kinetics and oxygen inhibition in dental adhesives.* Biomaterials, 2005. **26**(14): p. 1809-1817.

42. Roffey, C.G., *Photopolymerization of surface coatings*. 1982: Wiley.

43. Jeong, W., et al., *Hydrodynamic microfabrication via "on the fly" photopolymerization of microscale fibers and tubes.* Lab on a Chip, 2004. **4**(6): p. 576-580.

44. Noguchi, H., *Ink, ink-jet recording method using the same, and photopolymerization initiator*. 2002, Google Patents.

45. !!! INVALID CITATION !!! {}.

46. Hageman, H., *Photoinitiators for free radical polymerization.* Progress in organic coatings, 1985. **13**(2): p. 123-150.

47. Gruber, H., *Photoinitiators for free radical polymerization.* Progress in polymer Science, 1992. **17**(6): p. 953-1044.

48. Dadashi-Silab, S., C. Aydogan, and Y. Yagci, *Shining a light on an adaptable photoinitiator: advances in photopolymerizations initiated by thioxanthones.* Polymer Chemistry, 2015. **6**(37): p. 6595-6615.

49. Fouassier, J., X. Allonas, and D. Burget, *Photopolymerization reactions under visible lights: principle, mechanisms and examples of applications.* Progress in organic coatings, 2003. **47**(1): p. 16-36.

50. Dadashi-Silab, S., et al., *Magnetic iron oxide nanoparticles as long wavelength photoinitiators for free radical polymerization.* Polymer Chemistry, 2015. **6**(11): p. 1918-1922.

51. Tunc, D. and Y. Yagci, *Thioxanthone-ethylcarbazole as a soluble visible light photoinitiator for free radical and free radical promoted cationic polymerizations.* Polymer Chemistry, 2011. **2**(11): p. 2557-2563.

52. Wu, Q., et al., *Developing thioxanthone based visible photoinitiators for radical polymerization.* RSC Advances, 2014. **4**(94): p. 52324-52331.

53. Balta, D.K., et al., *Thioxanthone− Anthracene: A New Photoinitiator for Free Radical Polymerization in the Presence of Oxygen.* Macromolecules, 2007. **40**(12): p. 4138-4141.

54. Temel, G., et al., *Synthesis and characterization of one-component polymeric photoinitiator by simultaneous double click reactions and its use in photoinduced free radical polymerization.* Macromolecules, 2009. **42**(16): p. 6098-6106.

55. Temel, G., N. Arsu, and Y. Yagci, *Polymeric side chain thioxanthone photoinitiator for free radical polymerization.* Polymer Bulletin, 2006. **57**(1): p. 51-56.

56. Yamamoto, M. and G. Oster, *Zinc oxide-sensitized photopolymerization.* Journal of Polymer Science Part A-1: Polymer Chemistry, 1966. **4**(7): p. 1683-1688.

57. Hoffman, A., et al., *Photoinitiated polymerization of methyl methacrylate using Q-sized zinc oxide colloids.* The Journal of Physical Chemistry, 1992. **96**(13): p. 5540-5546.

58. Hoffman, A.J., et al., *Q-sized cadmium sulfide: synthesis, characterization, and efficiency of photoinitiation of polymerization of several vinylic monomers.* The Journal of Physical Chemistry, 1992. **96**(13): p. 5546-5552.

59. Strandwitz, N.C., et al., *One- and Two-Photon Induced Polymerization of Methylmethacrylate Using Colloidal CdS Semiconductor Quantum Dots.* Journal of the American Chemical Society, 2008. **130**(26): p. 8280-8288.

60. Zhang, D., et al., *Semiconductor nanoparticle-based hydrogels prepared via self-initiated polymerization under sunlight, even visible light.* Scientific Reports, 2013. **3**: p. 1399.

61. Andrzejewska, E. and M. Andrzejewski, *Polymerization kinetics of photocurable acrylic resins.* Journal of Polymer Science Part a-Polymer Chemistry, 1998. **36**(4): p. 665-673.

62. Tong, L. and W. Kenyon, *Heats of polymerization. I. An isothermal calorimeter and its application to methyl methacrylate.* Journal of the American Chemical Society, 1945. **67**(8): p. 1278-1281.

63. Criqui, A., et al., *Electron Spin Resonance Spin Trapping Technique: Application to the Cleavage Process of Photoinitiators.* Macromolecular Chemistry and Physics, 2008. **209**(21): p. 2223-2231.

64. Buettner, G.R., *Spin Trapping - Electron-Spin-Resonance Parameters of Spin Adducts.* Free Radical Biology and Medicine, 1987. **3**(4): p. 259-303.

65. Lagercrantz, C., *Spin trapping of some short-lived radicals by the nitroxide method.* The Journal of Physical Chemistry, 1971. **75**(22): p. 3466-3475.

66. Duling, D.R., *Simulation of multiple isotropic spin-trap EPR spectra.* J Magn Reson B, 1994. **104**(2): p. 105-10.

67. Stroyuk, A., V. Granchak, and S.Y. Kuchmii, *Polymerization of Butylmethacrylate in Isopropanol, Photoinduced by Quantum-Sized CdS Particles.* Theoretical and Experimental Chemistry, 2001. **37**(3): p. 174-179.

68. Decker, C. and K. Moussa, *Real-time kinetic study of laser-induced polymerization.* Macromolecules, 1989. **22**(12): p. 4455-4462.

69. Huang, Z.-Y., et al., *Heterogeneous photopolymerization of methyl methacrylate initiated by small ZnO particles.* The Journal of Physical Chemistry, 1994. **98**(48): p. 12746-12752.

70. Ojah, R. and S. Dolui, *Photopolymerization of methyl methacrylate using dye-sensitized semiconductor based photocatalyst.* Journal of Photochemistry and Photobiology A: Chemistry, 2005. **172**(2): p. 121-125.

71. Barichard, A., T. Galstian, and Y. Israëli, *Physico-chemical role of CdSe/ZnS quantum dots in the photo-polymerization process of acrylate composite materials.* Physical Chemistry Chemical Physics, 2012. **14**(22): p. 8208-8216.